

RESEARCH PAPER

Hot Jupiter - Cold Jupiter: A complex sibling relation

Adriana Errico,¹ Robert A. Wittenmyer,¹ Jonathan Horner,¹ Brad Carter,¹ and Valeria López²

¹University of Southern Queensland, Centre for Astrophysics, West Street, Toowoomba, QLD 4350, Australia

²Astronomy Department, Williams College, Williamstown, MA, 01267 USA

Author for correspondence: Adriana Errico, Email: aberrico@gmail.com.

(Received dd Mmm YYYY; revised dd Mmm YYYY; accepted dd Mmm YYYY; first published online 22 September 202X)

Abstract

A handful of planetary systems hosting a Hot Jupiter have been subsequently found to also host long-period giant planets. These “cold Jupiters,” giant planets residing beyond the snow line (~ 3 au), play an important role in the dynamical evolution of the system as a whole. In this work, we investigate the detectability of cold Jupiters around a sample of 28 well-studied Hot Jupiter host stars to estimate the occurrence rate of this distinctive system architecture. We perform extensive simulations using the combination of all publicly available radial velocity (RV) data for those stars with synthetic RV data. The synthetic data test observing strategies along three axes: cadence, duration, and measurement precision. For each scenario, we determine detection limits based on the semi-major axis at which a 1 Jupiter mass planet would be recovered 50% of the time. We find the following: 1) the existing RV data are remarkably insensitive to these Hot Jupiter/Cold Jupiter pairs; 2) the total baseline over which an observational campaign is carried out is the dominant factor in our ability to detect cold Jupiters; and 3) the results are relatively insensitive to the individual RV measurement precision. We conclude that metre-class telescopes with lower RV precision are ideally suited to surveying Hot Jupiter–cold Jupiter systems.

Keywords: Exoplanet astronomy (486) — Radial velocity (1332) — Hot Jupiters (753) — Exoplanet formation (492)

1. INTRODUCTION

Prior to the discovery of the first planets orbiting other stars, it was generally accepted that other planetary systems would resemble the Solar system. With the discovery of the first exoplanets, that assumption was revealed to be wholly incorrect – with the first detected planets (the pulsar planets, Draugh, Poltergeist and Phobetor/PSR B1257 +12 b, c, and d; and the first “Hot Jupiter” Dimidium/51 Pegasi b; Wolszczan & Frail, 1992; Wolszczan, 1994; Mayor & Queloz, 1995) proving utterly different to anything humanity had expected to find. Over the decades that followed, we discovered that the diversity of exoplanets was far greater than was ever anticipated based solely on our knowledge of the Solar system (e.g. Adams et al., 2016; Zhu et al., 2018a; Kunimoto & Matthews, 2020a)^a.

The discovery and characterisation of exoplanets has now matured to the point where, in an age where more than 5000 planets are known^b, we can make meaningful observational tests of key questions in planet formation. One such question is: How common (or unusual) are systems like the Solar system? This mystery has tickled the imaginations of humans since they first looked up at the stars and wondered whether there was another Earth out there. For the first time, the current generation of scientists has the data to quantitatively address this question. This endeavour is of vital importance because the coming decades will see the advent of extremely large

telescopes and flagship spacecraft missions designed to detect truly Earth-like planets in Earth-like orbits, and the search for life beyond the Solar system will begin in earnest (e.g. Horner & Jones, 2010; Fujii et al., 2018; Schwieterman et al., 2018; Harada et al., 2024a).

One issue confounding our attempts to place the Solar system in the context of the ‘typical’ exoplanetary system is that the techniques used to find the vast majority of known exoplanets are strongly biased towards the discovery of planetary systems that are very different to our own (see e.g. Perryman, 2018, and references therein). It is far easier to find massive planets orbiting close to their host stars than to find giant planets moving on decades-long orbits, like those seen in the Solar system. Similarly, detecting planets similar to the Solar system’s terrestrial worlds remains challenging – although as technology has improved over the years, such planets are now within our reach. Despite these challenges, however, a number of studies have been carried out attempting to bridge this gap, and to determine how common are planets analogous to Jupiter (e.g. Wittenmyer et al., 2016; Wittenmyer et al., 2020). The California Legacy Survey (Rosenthal et al., 2021) and the Kepler Giant Planet Survey (Weiss et al., 2024) are currently carrying out ongoing programs of RV observations to search for such planets.

Earth-size planets appear to be extremely common (e.g. Wittenmyer et al., 2011b; Dressing & Charbonneau, 2015; Zhu et al., 2018b; Kunimoto & Matthews, 2020b), and several tens of rocky planets are known to orbit in their host stars’ habitable zones (e.g. Gillon et al., 2017; Vanderburg et al., 2020; Gilbert et al., 2023). However, these orbital properties are merely a necessary, but not sufficient, condition for a planet to be

^aFor a detailed overview of the links between our knowledge of the Solar system and Exoplanetary Science, we direct the interested reader to Horner et al. (2020b), and references therein.

^bAt the time of writing (2026 Jan 2), the number of confirmed exoplanets listed on the NASA Exoplanet Archive (Christiansen et al., 2025) to date stands at 6,087.

genuinely Earth-like (see e.g. Horner & Jones, 2010, 2012; Waltham, 2019; Airapetian *et al.*, 2020; Horner *et al.*, 2020a; Vervoort *et al.*, 2022, and references therein). Occurrence rate studies suggest that there may be an embarrassment of riches in terms of potentially Earth-like planets, with some results indicating that frequency (eta-Earth) to be approaching unity (Bryson *et al.*, 2021) – though large uncertainties remain due to incompleteness. Choosing the best candidates will be a critical task in the years to come.

The presence of "Jupiter analogues": giant planets moving on low-eccentricity orbits beyond ~ 5 au (e.g. Wittenmyer *et al.*, 2011a; Zechmeister *et al.*, 2013; Wittenmyer *et al.*, 2016; Bonomo *et al.*, 2023), is thought to be a factor influencing the habitability of inner rocky planets (see e.g. Wetherill, 1994, 1995; Horner & Jones, 2008, 2009; Horner *et al.*, 2010; Graziop, 2016; Raymond & Izidoro, 2017; Vervoort *et al.*, 2022). The low eccentricities of such giant planets could indicate a relatively benign dynamical history for the system, enhancing the probability of an interior rocky planet remaining on a long-term stable, near-circular orbit like our Earth. Distant giant planets with high-eccentricity orbits are also of interest; cold giants that remain beyond the snow line are expected to have retained low-eccentricity orbits, unless perturbed by interactions with other planets. Such planet-planet scattering can result in ejections, or one planet being hurled into a highly elliptical orbit, and would also significantly destabilise the small bodies in the system – leading to periods of extreme impact rates on any terrestrial planet analogues (e.g. Gomes *et al.*, 2005; Levison *et al.*, 2011; Nesvorný, 2018), but potentially also delivering a wealth of volatile material to those planets (e.g. Owen & Bar-Nun, 1995; Morbidelli *et al.*, 2000; Horner *et al.*, 2009; O'Brien *et al.*, 2014; Raymond & Izidoro, 2017). These dynamical fingerprints are important evidence for determining the frequency of various outcomes of post-formation processes.

Systems containing highly eccentric cold giant planets are of particular interest as they tell an intriguing story of their misspent youth. Errico *et al.* (2022) reported the discovery of a giant planet with a 22-year orbital period and an eccentricity of $e = 0.76$ in the HD 83443 system, which was already known to host a Hot Jupiter (Butler *et al.*, 2002). This system configuration, with a Hot Jupiter and an eccentric distant cold Jupiter, is quite rare, with the HD 83443 system being only the eighth such system detected^c. The eccentric outer planet is thought to have originated from a dynamical event which scattered the Hot Jupiter inward while sending the outer planet into its highly elliptical orbit. The discovery naturally raises the question: How common is this outcome?

In this work, we examine all known Hot Jupiter systems which have publicly available radial velocity data, and ask how many "HD 83443-like" systems with an outer cold giant planet ("acquaintances of Hot Jupiters") could be lurking undetected. We model how future observations will impact the likelihood of finding cold giant planets of different masses at a variety of

distances, and examine the roles of observation cadence and instrumental precision on these results. Section 2 describes the extant observational data used to perform the simulations that are described in Section 3. Section 4 gives our results for 28 Hot Jupiter systems: both the current state of detectability for such Hot/Cold Jupiter systems, and the degree to which such planets would be detected under various observing scenarios. Finally in Section 5 we give our conclusions.

2. Observations

We selected the Hot Jupiters from the NASA Exoplanet Archive with the following criteria: orbital period < 10 days; semi-major axis < 0.1 au; and mass > 0.3 Jupiter mass (M_{Jup}). Because we are interested in radial velocity sensitivity to distant cold giant planets, we filtered our sample to include only those 37 Hot Jupiters that were discovered using that method. Whilst hundreds of Hot Jupiters are known from transit surveys, including them here would introduce a severe bias: such planets tend to be confirmed with only a short span of radial velocities, and hence their data would be useless in constraining the presence of long-period planets. We then obtained all publicly-available data from the Data & Analysis Center for Exoplanets (DACE database), a web platform at the University of Geneva dedicated to extrasolar planets data visualisation, exchange and analysis^d and from the HARPS RVBank (Trifonov *et al.*, 2020) for the planets in our sample.

Of the 37 Hot Jupiters discovered using the RV method, just 28 fulfil the criteria of having publicly available data – and thus these 28 planets form the final sample considered in this work. The observational data are summarised in Table 2, and can be graphically visualised in 1 and 2. As expected, the data come from disparate sources and time periods, hence they have offsets and gaps as visualised in Figures 1 and 2. Such features can affect the detectability of further planets; these subtleties have been explored in detail by other work (e.g. Wittenmyer *et al.*, 2013; Lagrange *et al.*, 2023; Li *et al.*, 2025). The main characteristics of the spectrographs selected for this analysis are summarised in Table 3

We note that we have carried out additional observations of HD 83443 using MINERVA-Australis (Wittenmyer *et al.*, 2018; Addison *et al.*, 2019; Addison *et al.*, 2021; Errico *et al.*, 2022) in the time since the 18-year Anglo-Australian Planet Search (Tinney *et al.*, 2001; Butler *et al.*, 2001; Wittenmyer *et al.*, 2014) ceased operation. Those data amount to 22 observations between 8 February 2019 to 22 February 2021.

^cThe other seven being: HD 118203, HD 187123, HD 217107, HD 68988, Pr0211, WASP-53, WASP-8. Star properties are summarised in Table 1.

^d<https://dace.unige.ch/dashboard/>

Table 1. Stellar properties of the eight stars currently known to host a hot Jupiter – cold Jupiter pair.

Star	Spectral type	Mass (M_{\odot})	Radius (R_{\odot})	T_{eff} (K)	[Fe/H]	Planet Reference	Parameter Reference
HD 68988	G1V	1.18	1.20	5978	+0.35	Rosenthal et al. (2021)	Grieves et al. (2018) Sousa et al. (2021)
HD 83443	K0V	0.97	1.02	5503	+0.34	Errico et al. (2022)	Cannon & Pickering (1993) Sousa et al. (2021)
HD 118203	G0V	1.35	1.99	5872	+0.27	Maciejewski et al. (2024)	Grieves et al. (2018) Sousa et al. (2021)
HD 187123	G2V	1.05	1.15	5837	+0.12	Wright et al. (2009)	Gray et al. (2001) Sousa et al. (2021)
HD 217107	G5V	1.06	1.12	5653	+0.35	Vogt et al. (2005a)	Cannon & Pickering (1993) Sousa et al. (2021)
Pr0211	G9V	0.935	0.827	5300	+0.18	Malavolta et al. (2016)	Kraus & Hillenbrand (2007) Malavolta et al. (2016)
WASP-53	K3V	0.80	0.93	4993	+0.23	Triaud et al. (2017)	Triaud et al. (2017) Sousa et al. (2021)
WASP-8	G8V	0.99	1.01	5627	+0.27	Knutson et al. (2014)	Salz et al. (2015) Sousa et al. (2021)

Table 2. Details of the archival data for the planet host systems featured in this work. The start and end dates for each data set are provided, along with the span across which observations were made (the observational baseline). The number of spectra and median precision of that data (in m/s) are given for each star, along with details of the instruments used. A graphical representation of the time coverage, including gaps and overlaps, for each target is given in Figs

Target	Start Date	End Date	Time Span (d)	# Spectra	Precision (m/s)	Instrument	Citation
BD-10 3166	1998 Dec 24	2000 Feb 11	464	84	3.69	HIRES	Butler et al. (2000)
	1998 Dec 24	2005 Jan 27	2226			HIRES	Butler et al. (2006)
	1998 Dec 24	2013 Dec 14	5469			HIRES	Butler et al. (2017)
HD 102956	2007 Apr 26	2013 Dec 13	2423	29	1.28	HIRES	Johnson et al. (2010)
HD 103720	2005 Feb 9	2014 April 16	3353	153	1.92	HARPS-pre ^e	Moutou et al. (2015)
	2005 Feb 9	2018 March 26	4793			HARPS-post	Trifonov et al. (2020)
HD 103774	2004 Dec 21	2012 July 11	2760	122	3.96	HARPS-pre	Lo Curto et al. (2013)
	2004 Dec 21	2018 April 2	4550			HARPS-post	Trifonov et al. (2020)
HD 11231	2015 Sep 21	2017 Jan 9	476	48	2.12	HARPS-post	Haswell et al. (2020)
HD 118203	2004 May 25	2005 July 1	402	99	14.72	ELODIE	da Silva et al. (2006)
	2004 May 25	2006 June 14	750			ELODIE	Castro-González et al. (2024)
HD 143105	2013 Jul 7	2014 set 2	422	100	9.18	SOPHIE+	Hébrard et al. (2016)
HD 120136 (Tau Boo)	1987 June 12	2002 Apr 6	5412	98	24.07	Lick	Butler et al. (1997, 2006)
HD 149026	2004 July 20	2004 Aug 24	35	98	1.86	HIRES	Sato et al. (2005)
	2005 Feb 27	2005 Aug 20	174			HIRES	Butler et al. (2006)
	2005 Feb 25	2014 Aug 26	3469			HIRES	Butler et al. (2017)
HD 149143	2005 June 28	2006 June 14	351	121	4.37	ELODIE	da Silva et al. (2006)
	2005 June 28	2005 Aug 31	64			ELODIE	da Silva et al. (2006)
	2004 July 11	2005 April 23	286			HIRES	Butler et al. (2006)
	2004 July 11	2014 Aug 23	3685			HIRES	Butler et al. (2017)
HD 162020	1999 June 24	2001 Oct 13	843	46	10.26	CORALIE	Udry et al. (2002)
HD 179949	1998 Sep 11	2006 June 25	2844	203	4.66	2.7m Tull	Tinney et al. (2001)
	2000 Sep 5	2000 Sep 8	3			HIRES	Tinney et al. (2001)
	2000 Sep 5	2005 June 25	1754			HIRES	Butler et al. (2006)
	2000 Sep 5	2014 Sep 8	5116			HIRES	Butler et al. (2017)

Continued on next page

^eWe note here that HARPS underwent a fibre upgrade in 2015 (as described in Lo Curto et al., 2015), with the result that data from before and after the change needs to be considered as data from two separate instruments. To make these data explicit, we therefore denote observations made before the change as HARPS-pre, and data after the change as HARPS-post.

Table 2 – continued from previous page

Target	Start Date	End Date	Time Span (d)	# Spectra	Precision (m/s)	Instrument	Citation
	1998 Nov 3	2000 Nov 7	735			UCLES	Tinney et al. (2001)
	1998 July 7	2005 Oct 27	2669			UCLES	Butler et al. (2006)
HD 185269	2005 June 30	2006 Aug 12	409	176	4.67	ELODIE	Johnson et al. (2006a)
	2005 June 30	2006 July 17	383			ELODIE	da Silva et al. (2006)
	2004 May 30	2006 June 18	749			Lick/Hamilton	Johnson et al. (2006a)
	2008 Dec 5	2014 Aug 22	2086			HIRES	Butler et al. (2017)
HD 187123	1998 Sep 30	2004 June 10	2079	453	4.19	ELODIE	Butler et al. (1998)
	1998 Sep 30	2003 Sep 5	1801			ELODIE	Naef et al. (2004)
	1997 Dec 23	1999 Sep 18	634			HIRES	Vogt et al. (2000)
	1997 Dec 23	2005 Dec 19	2918			HIRES	Butler et al. (2006)
	1997 Dec 23	2013 July 3	5671			HIRES	Feng et al. (2015)
	1997 Dec 23	2014 Sep 6	6101			HIRES	Butler et al. (2017)
HD 189733	2005 Aug 28	2006 Aug 12	349	309	1.74	ELODIE	Bouchy et al. (2005)
	2006 July 30	2007 Aug 29	395			HARPS	Triaud et al. (2009)
	2003 July 12	2006 Aug 21	1136			HIRES	Butler et al. (2006)
	2003 July 12	2014 Aug 24	4061			HIRES	Butler et al. (2017)
HD 209458	1999 June 26	2002 June 14	1084	551	7.33	CORALIE	Henry et al. (2000)
	1997 Aug 21	2006 Aug 13	3280			ELODIE	Naef et al. (2004)
	1997 Aug 21	2002 Oct 17	1884			ELODIE	Naef et al. (2004)
	1999 June 11	2004 Dec 31	2030			HIRES	Wittenmyer et al. (2005)
	1999 June 11	2002 Oct 28	1235			HIRES	Wittenmyer et al. (2005)
	1999 June 11	2005 Aug 22	2264			HIRES	Butler et al. (2006)
	1999 June 11	2014 Aug 19	5548			HIRES	Butler et al. (2017)
HD 212301	2003 Aug 5	2005 July 28	723	82	3.59	HARPS-Pre	Lo Curto et al. (2006)
HD 217107	1999 Sep 28	2005 Nov 15	2240	789	4.60	Lick/Hamilton	Fischer et al. (1999a)
	1998 Sep 11	1999 Dec 26	471			CORALIE	Naef et al. (2001)
	1998 Sep 11	1999 Dec 26	471			CORALIE	Feng et al. (2015)
	1998 July 11	1998 Dec 15	96			Lick/Hamilton	Fischer et al. (1999b)
	1998 Aug 2	2007 Nov 23	3400			Lick/Hamilton	Wright et al. (2009)
	1998 Jan 10	2003 May 17	51			Lick/Hamilton	Feng et al. (2015)
	1998 Sep 12	1998 Sep 19	7			HIRES	Fischer et al. (1999b)
	1998 Sep 12	1999 Sep 17	21			HIRES	Vogt et al. (2000)
	1998 Sep 12	2004 Dec 28	2299			HIRES	Vogt et al. (2005b)
	1998 Sep 12	2008 Sep 12	3653			HIRES	Wright et al. (2009)
	1998 Sep 12	2013 Dec 14	5572			HIRES	Feng et al. (2015)
	1998 Sep 12	2014 Sep 8	5840			HIRES	Butler et al. (2017)
HD 217014 (51Peg)	1994 Sep 15	2004 Dec 21	3751	730	6.45	ELODIE	Mayor & Queloz (1995)
	1994 Sep 15	2003 Sep 5	3277			ELODIE	Naef et al. (2004)
	1995 Oct 12	1996 Aug 31	324			Lick/Hamilton	Marcy et al. (1997)
	1995 Oct 12	2001 Oct 7	2187			Lick/Hamilton	Johnson et al. (2006a)
	2006 July 10	2014 Sep 13	2987			HIRES	Butler et al. (2017)
HD 2638	2003 Oct 31	2005 Jan 7	434	94	1.59	HARPS-Pre	Moutou et al. (2005)
HD 285507	2012 Sep 26	2013 Apr 4	32	190	12.15	TRES	Quinn et al. (2014)
HD 68988	1998 April 10	1998 May 13	33	98	2.63	HAMILTON	Vogt et al. (2002)
	1997 April 13	1998 Sep 8	513			HIRES	Vogt et al. (2002)
	1997 April 13	2006 Jan 18	2202			HIRES	Butler et al. (2006)
	1997 April 13	2014 Jan 18	5124			HIRES	Butler et al. (2017)
HD 75289	1998 Nov 13	1999 Oct 14	335	151	6.59	CORALIE	Udry et al. (2000)
	1998 Jan 16	2001 Jan 10	1090			UCLES	Butler et al. (2001)
	1998 Jan 16	2005 May 28	2689			UCLES	Butler et al. (2006)
HD 83443	1999 March 25	2003 March 19	1455	147	2.75	CORALIE	Butler et al. (2002)
	1998 March 25	1999 June 5	437			HIRES	Vogt et al. (2002)
	1998 March 25	2005 Feb 25	1529			HIRES	Butler et al. (2006)
	1998 March 25	2014 Dec 11	5105			HIRES	Butler et al. (2017)
	2019 Feb 8	2019 Feb 23	15			Minerva-ThAr	Errico et al. (2022)
	2021 Feb 17	2021 Feb 22	5			Minerva-Iodine	Errico et al. (2022)
	2003 Dec 28	2015 May 1	4142			HARPS-pre	Moutou et al. (2015)
	2015 Dec 10	2016 May 28	170			HARPS-post	Trifonov et al. (2020)
	1999 Feb 2	2015 March 13	5883			UCLES	Tinney et al. (2001)

Continued on next page

Table 2 – continued from previous page

Target	Start Date	End Date	Time Span (d)	# Spectra	Precision (m/s)	Instrument	Citation
HD 86081	2005 Nov 19	2006 Feb 14	87	73	2.06	HIRES	Butler et al. (2006)
	2005 Nov 19	2013 Dec 14	2947			HIRES	Butler et al. (2017)
HD 88133	2004 Jan 10	2004 July 13	185	114	2.19	HIRES	Fischer et al. (2005)
	2004 Jan 10	2005 April 23	469			HIRES	Butler et al. (2006)
	2004 Jan 10	2014 Jan 19	3662			HIRES	Butler et al. (2017)
HD 9826 (Ups And)	1994 Sep 22	1999 Feb 4	1596	1143	8.57	AFOE	Butler et al. (1997)
	1999 Oct 1	2006 Jan 11	2294			Hobby-Eberly	Wittenmyer et al. (2007)
	1996 Aug 23	2006 Aug 13	3641			ELODIE	Mayor & Queloz (1995)
	1996 Aug 23	2003 Sep 3	2566			ELODIE	Naef et al. (2004)
	1987 Sep 8	1999 March 5	4196			Lick/Hamilton	Fischer et al. (1999b)
	1987 Sep 8	2002 Nov 19	5551			Lick/Hamilton	Fischer et al. (2003)
	1987 Sep 8	2004 Aug 3	6174			Lick/Hamilton	Butler et al. (2006)
1994 Nov 24	2007 Nov 24	4748	Lick/Hamilton	Wright et al. (2009)			
HIP 14810	2005 Nov 19	2006 Sep 6	291	176	1.12	HIRES	Butler et al. (2006)
	2005 Nov 19	2008 Dec 5	1112			HIRES	Wright et al. (2009)
	2005 Nov 19	2014 Aug 5	3178			HIRES	Butler et al. (2017)

Table 4 summarises the stellar parameters for our 28 target stars. Table 5 shows the planetary parameters of the Hot Jupiter for each of our targets. The host stars considered here are generally mature Solar-type dwarfs, reflecting the selection biases of radial velocity surveys. The specific selection functions of the multifarious RV surveys included herein are beyond the scope of this work – but in general they tend to select solar type, quiet, single stars as represented in Table 4. Such stars are therefore well-represented in the exoplanet demographics literature, with cold giant planets found to orbit $\sim 10\%$ of them (e.g. Cumming et al., 2008; Wittenmyer et al., 2011a; Zechmeister et al., 2013; Bryan et al., 2016; Wittenmyer et al., 2016; Nielsen et al., 2019; Poleski et al., 2021; Gan et al., 2024). The effect of the presence of a Hot Jupiter on the occurrence rate of cold Jupiters is unexplored and is the main aim of this work.

3. Methodology

In this section, we describe the two main analysis procedures employed to assess the current and future detectability of long-period "acquaintances" to the known Hot Jupiters studied in this work. First, we examine the sensitivity afforded by the existing data. Then, we perform a suite of simulations under various scenarios of instrumental precision, observing cadence, and temporal baseline. Taken together, these analyses reveal the extent of our knowledge about such cold giant companions and inform the observational strategies required to probe the outer reaches of these planetary systems.

3.1 Existing Data

To assess the sensitivity of the existing data to cold Jupiters, we conducted injection-recovery tests using *RVSearch* (Rosenthal et al., 2021), a Python package built on top of *RadVel* (Fulton et al., 2018). The algorithm injects synthetic planetary signals, with orbital periods and minimum masses ($m \sin i$) drawn from log-uniform distributions, eccentricities that are drawn from a beta distribution (Kipping, 2013), and the argument of periapsis drawn from uniform distribution between 0 and 360° . It is assumed that the orbits of the planets are co-planar in this injection analysis. *RVSearch* then attempts to recover each injected signal, estimating the detection probability for planets across a range of parameters. As a graphic output, the algorithm produces a completeness contour plot featuring two clearly distinct regions, as illustrated for HD 103720 in Figure 3.

RVSearch has become a widely adopted tool in the exoplanet community, particularly for evaluating survey completeness and population-level detection efficiencies (Howard & Fulton, 2016; Fulton et al., 2018; Rosenthal et al., 2021). Its performance has been validated across diverse RV datasets (e.g. Polanski et al., 2024; Zhang et al., 2025; Van Zandt et al., 2025), and it has been instrumental in quantifying detection biases and uncovering the parameter space accessible to current surveys (e.g. Laliotis et al., 2023; Harada et al., 2024b; Wittenmyer et al., 2025). A detailed technical description of the algorithm, including its treatment of multi-instrument datasets

and inter-dataset offsets, is provided in (Rosenthal et al., 2021), to which we refer the reader for full details. For our analysis, we employed the standard *RVSearch* configuration, with 3000 injected trial signals per star to ensure convergence of the completeness estimates. Tests with larger numbers of injections yielded consistent results, supporting the robustness of this choice, but proved to be prohibitively computationally intensive for such injection numbers to be used for our full analysis. Poorly sampled or highly eccentric orbital configurations are naturally incorporated into the injection-recovery framework, and their contribution to the overall completeness is therefore properly accounted for.

3.2 Simulated Data

To inform the observational strategy, we tested nine scenarios in a 3×3 grid of (low, medium, high) cadence^f and (low, medium, high) RV measurement precision. We define these categories of measurement precision by representative instruments: "low" – *MINERVA-Australis* (Addison et al., 2019), "medium" – *Keck/HIRES* (Vogt et al., 1994), "high" – *VLT/ESPRESSO* (Pepe et al., 2014). We wish to test the relative importance of precision and cadence for this science goal, and these values of cadence and precision for the simulated observations are chosen to bracket the range of typical RV survey programmes. Clearly, one would like to observe at the highest cadence and the highest precision, but the realities of telescope time allocation preclude such a scenario. In general, precision and cadence (i.e. the amount of time available) are inversely related. Small telescopes, such as those that make up the *MINERVA-Australis* array (Addison et al., 2019), can dedicate a great deal of time to such a project, whereas larger telescopes with more in-demand instruments (e.g. *Keck/HIRES*, *VLT/ESPRESSO*) would naturally be under far more competitive pressure, limiting the available time.

To test the relative importance of these factors, we simulate observing campaigns for the 28 stars examined herein. We also test three different temporal baselines for the new observations: 3, 6, and 12 years. The purpose is to determine the degree to which the observational baseline can overcome lower cadence and/or instrumental precision. The final result is a set of 27 total observing scenarios for each of our 28 selected systems. Since it is not possible to include such a large number of figures, we include Figure 5 to illustrate the improvement in detection when comparing low- and high-cadence observations for the three selected telescopes. Again, it is obvious that the highest cadence, at the highest precision, for the longest time, will always produce the best results. Our purpose here is to provide a matrix of possibilities to inform and optimise observing strategies to address the science goal of measuring the occurrence rate of Hot Jupiter-Cold Jupiter pairs.

We generated simulated RVs using the fitted parameters of the known planet(s) to produce Keplerian orbits, to which

^flow cadence – 4 observations per year (approximately every two months)
 medium cadence – 8 observations per year (approximately every month)
 high cadence – 16 observations per year (approximately twice a month)

RV Data Time Sampling for Hot Jupiter Systems (Part 1/2)
(Datasets at Integer Y-levels by First Observation Date)

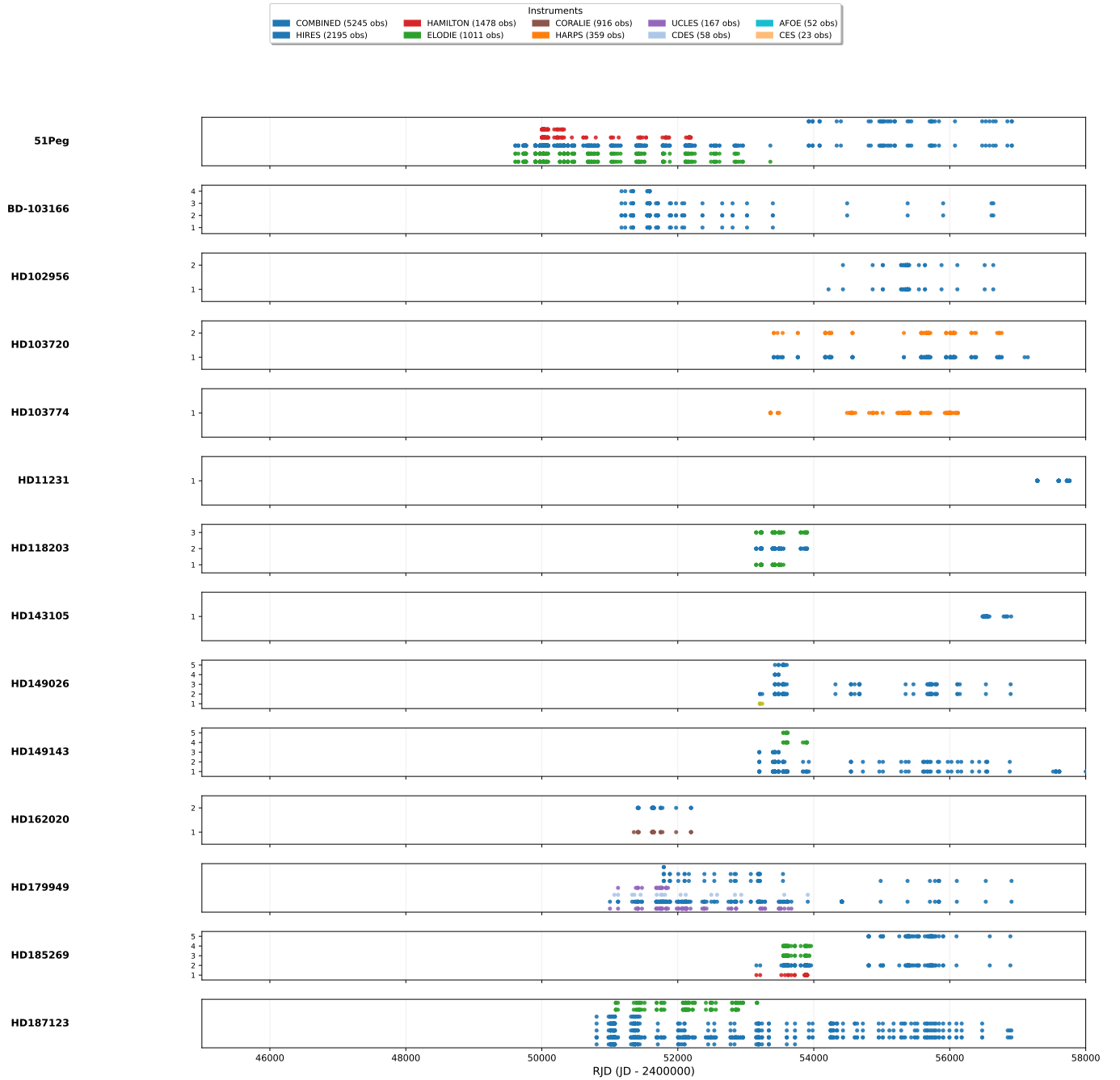


Figure 1. The distribution of RV data used in this work over time for the selected targets (part 1). The instrumental precision of this data, along with additional data, are presented in Table 2.

Table 3. Instrumental parameters of selected Telescopes.

Instrument	Wavelength range (nm)	Resolving power (R)	Precision (m s ⁻¹)	Telescope & Size
VLT/ESPRESSO	380-788	70,000 (4-UT), 140,000–190,000 (1-UT)	0.1	VLT UT, 8.2 m (single UT) / equiv. 16 m (4-UT)
Keck/HIRES	370-800	~60,000	3	Keck, 10 m
MINERVA-Australis	480-630	≥75,000	10	4×0.7 m CDK700

RV Data Time Sampling for Hot Jupiter Systems (Part 2/2)
(Datasets at Integer Y-levels by First Observation Date)

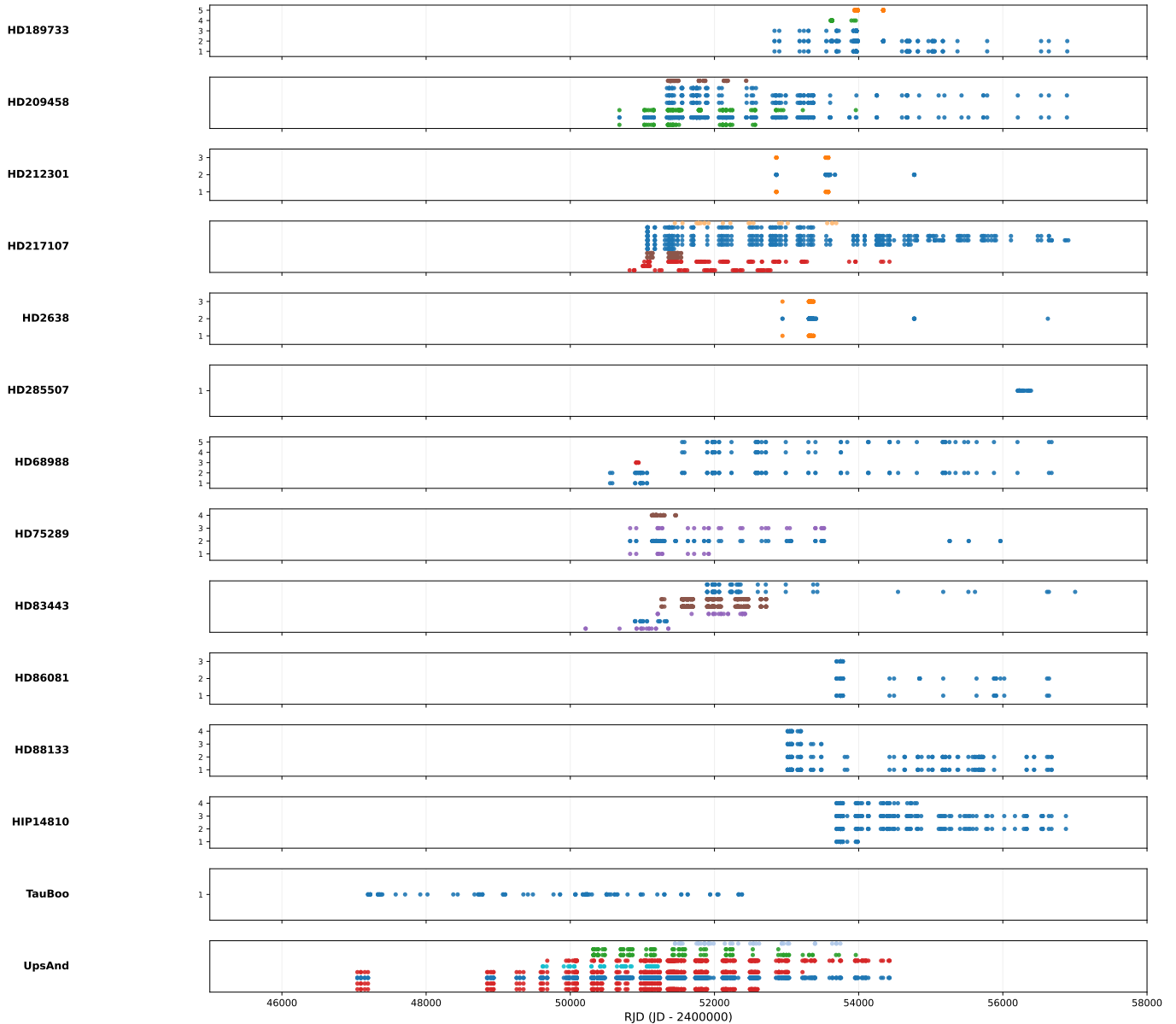


Figure 2. The distribution of RV data used in this work over time for the selected targets (part 2). The instrumental precision of this data, along with additional data, are presented in Table 2.

Table 4. Stellar parameters of selected host stars. For consistency, all parameters listed here are sourced from Sousa et al. (2021), though we note that they have been rounded for ease of reading.

Star	V_{mag}	Mass (M_{\odot})	T_{eff} (K)	$\log g$ (cgs)	[Fe/H]
51 Peg (HD 217014)	5.46	1.07	5810	4.33	+0.21
BD-10 3166	10.01	0.94	5417	4.32	+0.34
HD 102956	7.85	1.48	5010	3.21	+0.10
HD 103720	9.49	0.75	4914	4.21	-0.02
HD 103774	7.12	1.43	6586	4.48	+0.31
HD 11231	8.57	1.49	6643	4.32	+0.19
HD 118203	8.06	1.35	5872	4.05	+0.27
HD 143105	6.75	1.35	6381	4.41	+0.17
HD 149026	8.14	1.32	6166	4.35	+0.37
HD 149143	7.89	1.31	5958	4.20	+0.33
HD 162020	9.12	0.72	4751	4.26	-0.06
HD 179949	6.25	1.24	6282	4.49	+0.23
HD 185269	6.68	1.37	6063	4.09	+0.16
HD 187123	7.83	1.05	5837	4.37	+0.12
HD 189733	7.68	0.75	4969	4.30	-0.08
HD 209458	7.63	1.12	6126	4.50	+0.04
HD 212301	7.76	1.22	6261	4.49	+0.20
HD 217107	6.18	1.06	5653	4.28	+0.35
HD 2638	9.38	0.84	5230	4.35	+0.15
HD 285507	10.50	0.69	4523	4.14	+0.10
HD 68988	8.19	1.18	5978	4.54	+0.35
HD 75289	6.36	1.25	6181	4.40	+0.30
HD 83443	8.24	0.97	5503	4.30	+0.34
HD 86081	8.70	1.29	6057	4.22	+0.27
HD 88133	8.06	1.23	5469	3.91	+0.36
HIP 14810	8.50	1.00	5638	4.40	+0.28
τ Boo	4.49	1.46	6735	4.79	+0.39
υ And	4.10	1.34	6275	4.29	+0.20

Table 5. Orbital parameters of hot Jupiter exoplanets used in this work. For each system, we present the parameters as derived in the discovery work, for consistency. Where the discovery work does not provide a given parameter, we give the value presented by the next available work, for completeness. Where no uncertainties were presented, we give the value as published. We note that these numbers are presented solely for the benefit of the reader, as our analysis fully refit each system rather than assuming a prior published orbit for known planets.

Planet	$M \sin i (M_{\text{Jup}})$	a (AU)	e	Period (days)	K (m/s)	Citation
51 Peg b	0.472 ± 0.039	0.0527 ± 0.0030	0.013 ± 0.012	4.230785 ± 0.000036	55.94 ± 0.69	Mayor & Queloz (1995)
HD 189733 b	1.15 ± 0.04	0.0313 ± 0.0004	0	2.219 ± 0.0005	205 ± 6	Bouchy et al. (2005)
HD 209458 b	0.63	0.0467	0.00 ± 0.04	3.5250 ± 0.003	81.5 ± 5.5	Charbonneau et al. (2000) Henry et al. (2000)
τ Boo b	3.87	0.0462	0.018 ± 0.016	3.3128 ± 0.0002	469 ± 5	Butler et al. (1997)
υ And b	0.68	0.057	0.109 ± 0.040	4.611 ± 0.005	74.1 ± 4.0	Butler et al. (1997)
HD 75289 b	0.42	0.046	0.024 ± 0.021	3.5098 ± 0.0007	54 ± 1	Udry et al. (2000)
HD 83443 b	0.34	0.0375	0.0520 ± 0.0500	2.98553 ± 0.00040	57.5 ± 0.2	Butler et al. (2002)
HD 179949 b	0.84 ± 0.05	0.045 ± 0.004	0.05 ± 0.03	3.093 ± 0.001	102.2 ± 3.0	Tinney et al. (2001)
HD 187123 b	0.52	0.042	0.03 ± 0.03	3.097 ± 0.03	72.0 ± 2.0	Butler et al. (1998)
HD 149026 b	0.36 ± 0.03	0.042	0	2.8766 ± 0.001	43.3 ± 1.2	Sato et al. (2005)
BD-10 3166 b	0.48 ± 0.03	0.046	0.05 ± 0.05	3.487 ± 0.001	60.6 ± 1.01	Butler et al. (2000)
HD 102956 b	0.96 ± 0.05	0.081 ± 0.002	0.048 ± 0.027	6.4950 ± 0.0004	73.7 ± 1.9	Johnson et al. (2010)
HD 103720 b	0.620 ± 0.025	0.0498 ± 0.0008	0.086 ± 0.024	4.5557 ± 0.0001	89 ± 2	Moutou et al. (2015)
HD 103774 b	0.367 ± 0.022	0.070 ± 0.001	0.09 ± 0.04	5.8881 ± 0.0005	34.3 ± 1.8	Lo Curto et al. (2013)
DMPP 2-b (HD 11231 b)	$0.437^{+0.030}_{-0.059}$	0.0664 ± 0.0005	0.078	$5.2072^{+0.0002}_{-0.0055}$	$40.26^{+2.69}_{-5.34}$	Haswell et al. (2020)
HD 118203 b	2.13	0.07	0.309 ± 0.014	6.1335 ± 0.0006	217.0 ± 3.0	da Silva et al. (2006) Stassun et al. (2017)
HD 143105 b	1.21 ± 0.06	0.0379 ± 0.0009	<0.07	2.1974 ± 0.0003	144.0 ± 2.6	Hébrard et al. (2016)
HD 149143 b	1.33	0.053	0.016 ± 0.01	4.072 ± 0.70	149.6 ± 3.0	Fischer et al. (2006)
HD 162020 b ^a	14.4	0.074	0.277 ± 0.002	8.428198 ± 0.000056	1813 ± 4	Udry et al. (2002)
HD 185269 b	0.94	0.077	0.30 ± 0.04	6.838 ± 0.001	91 ± 4.5	Johnson et al. (2006b)
HD 212301 b	0.450	0.03600	0.000	2.245715 ± 0.000028	59.5 ± 0.7	Lo Curto et al. (2006) Stassun et al. (2017)
HD 217107 b	1.37 ± 0.14	0.074 ± 0.002	0.13 ± 0.02	7.1269 ± 0.00022	140.7 ± 2.6	Vogt et al. (2005a)
HD 2638 b	0.48	0.044	0.0	3.4442 ± 0.0002	67.4 ± 0.4	Moutou et al. (2005)
HD 285507 b	0.917 ± 0.033	0.060 ± 0.000	0.086 ± 0.019	6.0881 ± 0.0018	125.8 ± 2.3	Quinn et al. (2014) Stassun et al. (2017)
HD 68988 b	1.9	0.071	0.14 ± 0.03	6.276 ± 0.002	187 ± 6	Vogt et al. (2002)
HD 86081 b	1.50	0.035	0.0080 ± 0.0040	2.1375 ± 0.0002	207.7 ± 0.8	Johnson et al. (2006b)
HD 88133 b	0.29	0.046	0.11 ± 0.05	3.415 ± 0.001	35.7 ± 2.2	Fischer et al. (2005)
HIP 14810 b	3.84 ± 0.54	0.0692 ± 0.0040	0.1480 ± 0.0060	6.6740 ± 0.0020	420.7 ± 3.0	Butler et al. (2006)

^aWe note here that the mass determined for HD 162020 b in the discovery work is greater than $13 M_{\text{Jup}}$, and, as such, that object might well be considered to be a brown dwarf rather than a giant planet. Regardless of its true nature, we have included the system in this work for completeness. It should also be noted that more recent work (Stassun et al., 2017) obtains a planetary mass for this object, at $M \sin i$ of $9.840 \pm 2.750 M_{\text{Jup}}$.

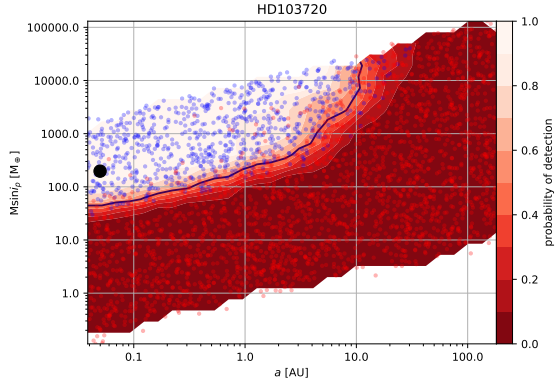


Figure 3. RVSearch completeness contour plot for HD 103720. The large black dot represents the periodic signal identified by RVSearch (i.e., the known planet). The small points denote injected synthetic planets. Blue points correspond to recovered signals, while red points were not recovered. Red contours show the detection probability, averaged over small bins in semi-major axis and $m \sin i$ space. The black line marks the 50% detection probability contour.

noise was added. The value of the noise was drawn with replacement from the residuals of a fit to the known planet(s) performed with the DACE tool (Fulton et al., 2018). We draw the uncertainty of each simulated measurement from a Gaussian distribution with means and standard deviation as follows in units of m s^{-1} : "low precision": $\mu = 10$ and $\sigma = 2$; "medium precision": $\mu = 3$ and $\sigma = 0.6$; "high precision": $\mu = 0.5$ and $\sigma = 0.1$. These were chosen to approximate, respectively, instruments akin to MINERVA and MINERVA-Australis (Swift et al., 2015; Wilson et al., 2019; Addison et al., 2019), Keck/HIRES (Vogt et al., 1994), and VLT/ESPRESSO (Pepe et al., 2014). Hereafter we refer to these instruments by name as exemplars of the three levels of measurement precision tested.

4. Results

In this section, we present the results of our detection sensitivity analysis for the currently available data, then show the results of the simulated scenarios to illustrate the effectiveness of various instruments and observing strategies.

4.1 Sensitivity of existing data to cold giant companions

Despite these being well-studied and bright Hot Jupiter hosts, the existing data are remarkably ineffective at detecting cold Jupiters (Table 6). Figure 4 shows the detection sensitivity for cold Jupiters averaged over our 28 Hot Jupiter systems. From these results, we see that in general, 49.91 percent of cold Jupiters beyond 3 au ($P \sim 5$ years) could be detected with the currently available data. To aid in interpreting the heat maps in this Section, we note that the typical uncertainty of the location of the RVSearch 50% recovery boundary (as denoted by the thick black line in Figure 3) is about 10% in semimajor axis space. Furthermore, it is worth noting that RVSearch correctly identified the known Hot Jupiter in 98.8% of trials.

Zink & Howard (2023) presented a completeness-corrected occurrence rate for Hot Jupiter-Cold Jupiter pairs of nearly 100%, with a steeply rising power-law toward longer periods. The extremely low completeness shown in our sample is consistent with this interpretation: that such "acquaintances of Hot Jupiters" should be common (approaching 100%) but a great many have so far been missed. To better understand these systems and their architectures, it is therefore profitable to continue to observe these systems. In the next subsection, we show the results of our simulated observing strategies designed to identify the most efficient route to reveal the population of these cold companions lurking in the outer darkness.

4.2 Nine Future Observation Scenarios for Three Different Exoplanet Observation Facilities

In Figure 6, we summarise the results of our simulated scenarios for each of the three observatories considered in this work (MINERVA/MINERVA-Australis, Keck/HIRES, and VLT/ESPRESSO). In each panel, we present a three-by-three grid showing the semi-major axis at which the facility has a 50% chance of recovering a $1 M_{\text{Jup}}$ planet for each combination of observing cadence (low, medium, high) and baseline of additional observations (3, 6, or 12 years)[§]. Each box represents the mean semi-major axis across the 28 stars in our sample. The three facilities in the figure are characterised by assumed instrumental RV precisions of 10 m s^{-1} for MINERVA-Australis – Figure 6a; 3 m s^{-1} for Keck/HIRES – Figure 6b; and 0.5 m s^{-1} for VLT/ESPRESSO – Figure 6c. For reference, the complete data for each telescope, for each combination of cadence and duration are given in Tables 7, 8 and 9

The first detail to notice is that for lower cadence and shorter duration, the semi-major axis at which a $1 M_{\text{Jup}}$ planet is detectable is smaller than for scenarios with higher cadence and longer duration, as one would intuitively expect. The second detail regarding the comparison of telescopes is that the highest-precision instrument detects a $1 M_{\text{Jup}}$ planet at a larger semi-major axis than lower-precision instruments for a given combination of cadence and duration; this is again consistent with expectations. However, it is perhaps surprising to note that the gains made from greatly improved RV precision are only small, compared to those accrued as a result of longer baselines or higher observation cadence.

Indeed, it is particularly interesting that the detection semi-major axis achieved by the facility with the lowest RV precision (MINERVA-Australis) for combinations of higher cadence and longer durations equals or exceeds the performance of more precise instruments at lower cadence and/or shorter durations. These results show that the disadvantage of lower measurement precision can be compensated for by higher cadence – demonstrating the ongoing value of "regular" RV observations in an extreme-precision (EPRV) world. In other words, an VLT/ESPRESSO-like EPRV instrument may deliver measurement precision 10–20 times better than a MINERVA-Australis-

[§]These values correspond to the semi-major axis of the thick black contour in the exemplar results from RVSearch, shown in Figure 3, for a mass of $1 M_{\text{Jup}}$

Table 6. Semi-major axes (in AU) at which 50% of $1 M_J$ planets would be detected, should they be present in the system in question, based upon an injection-recovery analysis of the currently available radial velocity data. The data reveals significant differences in our ability to detect Cold Jupiters across this population of 28 stars for which long-period radial velocity data are available.

Target	semi-major axis (AU)
51Peg	5.85
BD-10 3166	2.69
HD102956	1.28
HD103720	2.31
HD103774	0.98
HD11231	0.10
HD118203	0.57
HD143105	0.44
HD149026	2.01
HD149143	2.60
HD162020	1.07
HD179949	1.17
HD185269	3.49
HD187123	9.98
HD189733	0.52
HD209458	6.21
HD212301	0.72
HD217107	9.09
HD2638	0.60
HD285507	0.59
HD68988	2.81
HD75289	4.90
HD83443	7.57
HD86081	1.11
HD88133	3.76
HIP14810	2.27
TauBoo	0.10
UpsAnd	2.34

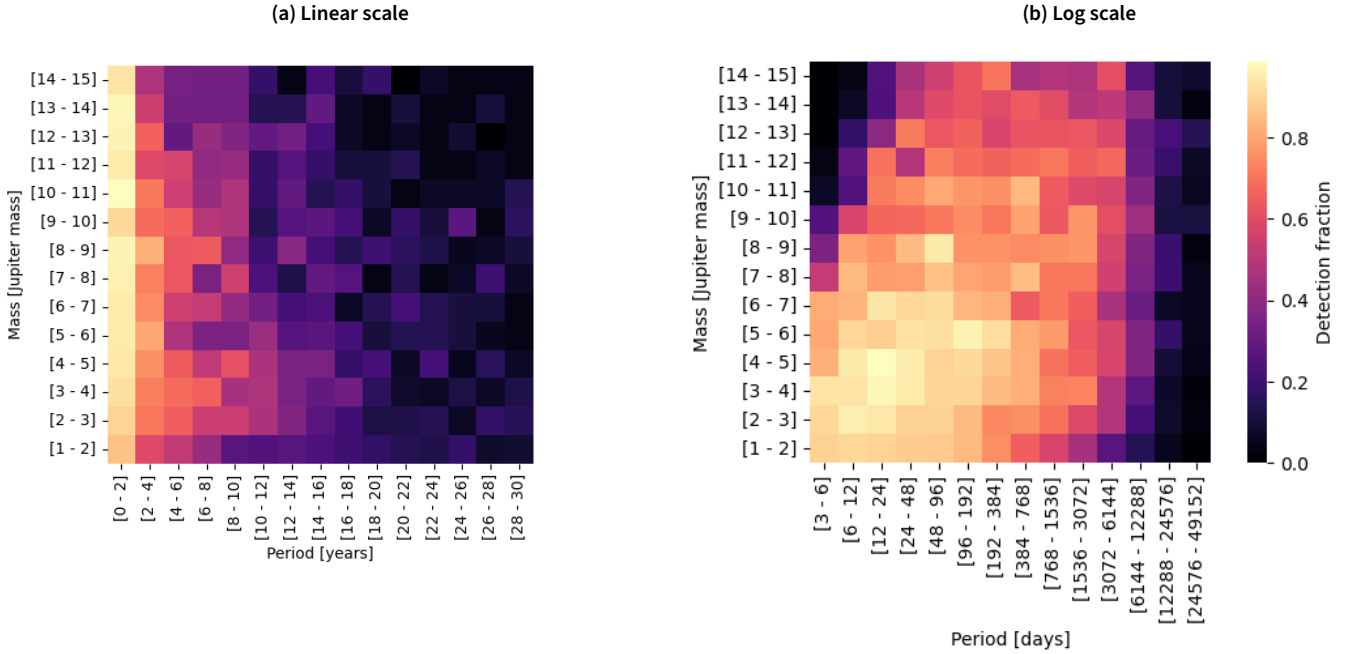


Figure 4. Heat maps showing the detection efficiency for exoplanet candidates injected to the existing observational radial velocity data for 28 known Hot Jupiter host stars. A total of 3,000 unique potential candidate companions were injected, one at a time, for each star considered, with masses and orbital periods each drawn from a log-normal distribution. In both panels, the colour of a square denotes the detection efficiency for a planet in that square – the mean of the detection efficiencies (number of detections divided by the number of injected planets) across the sample of 28 stars. The left panel shows the data as a function of orbital period, whilst the right shows the same data as a function of $\log(\text{period})$. It is clear that planets are most easily detected at short orbital periods, with true Jupiter and Saturn analogues ($P \sim 12$ and 29 years, respectively) challenging to detect based on current data. The “void” at the top left of the right hand panel is an artefact of the injection-recovery process; the signals injected by RVSearch all had radial velocities of less than 1000 m s^{-1} . As a result, no planets were generated in the region of the ‘void’, and so recovery of planets in that region was impossible as there were none to recover.

like facility, but, when those facilities are used to search for Cold Jupiters, the “lesser” (and more accessible) facility achieves the desired outcome.

For each star (and each scenario), RVSearch produces a table containing the orbital parameters of the injected signals (planets) and whether they were recovered. We considered the space defined by planet mass and period and divided it into “boxes” (for example, intervals of one Jupiter mass and two years). As an illustration, the first box (located at the bottom left of the heat map in Figure 4) spans from 1 to 2 Jupiter masses and from 0 to 2 years. The right panel (Figure 4) shows the same result on a log scale.

It is interesting to directly compare the characteristics of the real observational data (presented in Figure 4) and the simulated data (Figure 7). The high degree of similarity between the two figures is encouraging – revealing that the simulated data has very similar characteristics to the real data. In other words, this suggests that the methodology behind the creation of the simulated data is robust, and accurately reflects the reality of the observations made.

For each mass–period box, we computed the ratio of detected to injected signals (this ratio is always less than or equal to 1) and visualised the results as a heat map. This process yielded 756 heat maps, which we then averaged box-by-box across all stars, resulting in 9 heat maps that represent the average detection rates over the 28 stars.

Table 7. Table showing the semi-major axis (in AU) at which a detection efficiency of 50% is achieved for 1 M_J planets orbiting the 28 targets stars of this study, for a low-precision, MINERVA-Australis analogue facility, as a function of the observational baseline and observational cadence used. In general, the longer the observation baseline, the more distant the Jupiter analogues that could be detected, regardless of the observation cadence chosen. However, it is clear that, for most targets, applying a higher cadence yields markedly better results than simply observing with low cadence.

	Low cadence			Medium cadence			High cadence		
	3 years	6 years	12 years	3 years	6 years	12 years	3 years	6 years	12 years
51Peg	5.87	5.74	5.99	5.85	5.87	5.87	5.85	5.91	6.52
BD-10 3166	3.0	2.96	3.96	3.09	3.91	5.71	3.51	4.92	7.37
HD102956	0.97	1.08	0.84	1.14	0.95	1.2	0.98	1.1	1.22
HD103720	2.56	2.36	2.56	2.37	2.49	2.66	2.43	2.82	4.8
HD103774	0.95	1.06	1.16	0.96	1.17	1.15	1.06	1.16	1.78
HD11231	0.1	0.36	0.46	0.35	0.54	0.56	0.64	1.16	3.14
HD118203	0.14	0.15	0.18	0.15	0.18	0.19	0.19	0.18	0.21
HD143105	0.49	0.51	0.55	0.52	0.55	0.59	0.65	0.64	0.91
HD149026	2.54	3.27	4.72	2.51	4.54	7.76	4.28	5.96	8.21
HD149143	2.73	2.82	2.82	2.7	2.94	3.32	2.92	2.72	4.79
HD162020	1.13	1.15	0.1	1.08	0.11	0.1	0.13	0.1	0.1
HD179949	1.15	1.2	1.21	1.18	1.14	1.17	1.23	1.18	1.1
HD185269	3.62	3.32	3.62	3.4	1.67	1.84	1.79	1.84	1.86
HD187123	1.85	10.57	9.97	2.0	2.09	2.02	10.29	9.73	7.62
HD189733	0.67	0.78	0.79	0.9	0.8	1.05	0.82	1.2	1.14
HD209458	6.18	6.35	6.12	6.03	6.25	7.29	6.21	6.37	7.72
HD212301	0.7	1.08	1.82	0.91	1.69	2.62	1.84	1.97	5.71
HD217107	6.41	8.51	8.91	8.27	9.31	9.24	9.16	9.29	8.79
HD2638	0.62	0.69	0.68	0.66	0.59	1.65	0.7	2.58	7.13
HD285507	1.36	1.05	1.04	1.4	1.77	4.22	1.78	1.99	6.55
HD68988	2.87	3.43	3.04	3.23	3.14	0.26	3.35	0.2	0.24
HD75289	3.23	4.55	5.48	4.74	5.1	6.49	4.88	6.49	8.4
HD83443	7.79	7.22	6.32	8.15	7.36	7.98	7.56	4.4	5.02
HD86081	1.2	1.2	0.89	1.37	1.19	1.45	1.25	2.49	6.28
HD88133	4.26	4.73	5.32	4.3	5.18	6.76	4.77	6.29	8.19
HIP14810	2.6	2.55	2.58	2.54	2.42	2.97	2.58	2.89	2.63
TauBoo	0.1	0.1	0.1	0.1	0.1	0.1	0.1	0.1	0.1
upsAnd	2.28	2.42	2.18	2.17	2.36	2.5	2.42	2.48	2.33

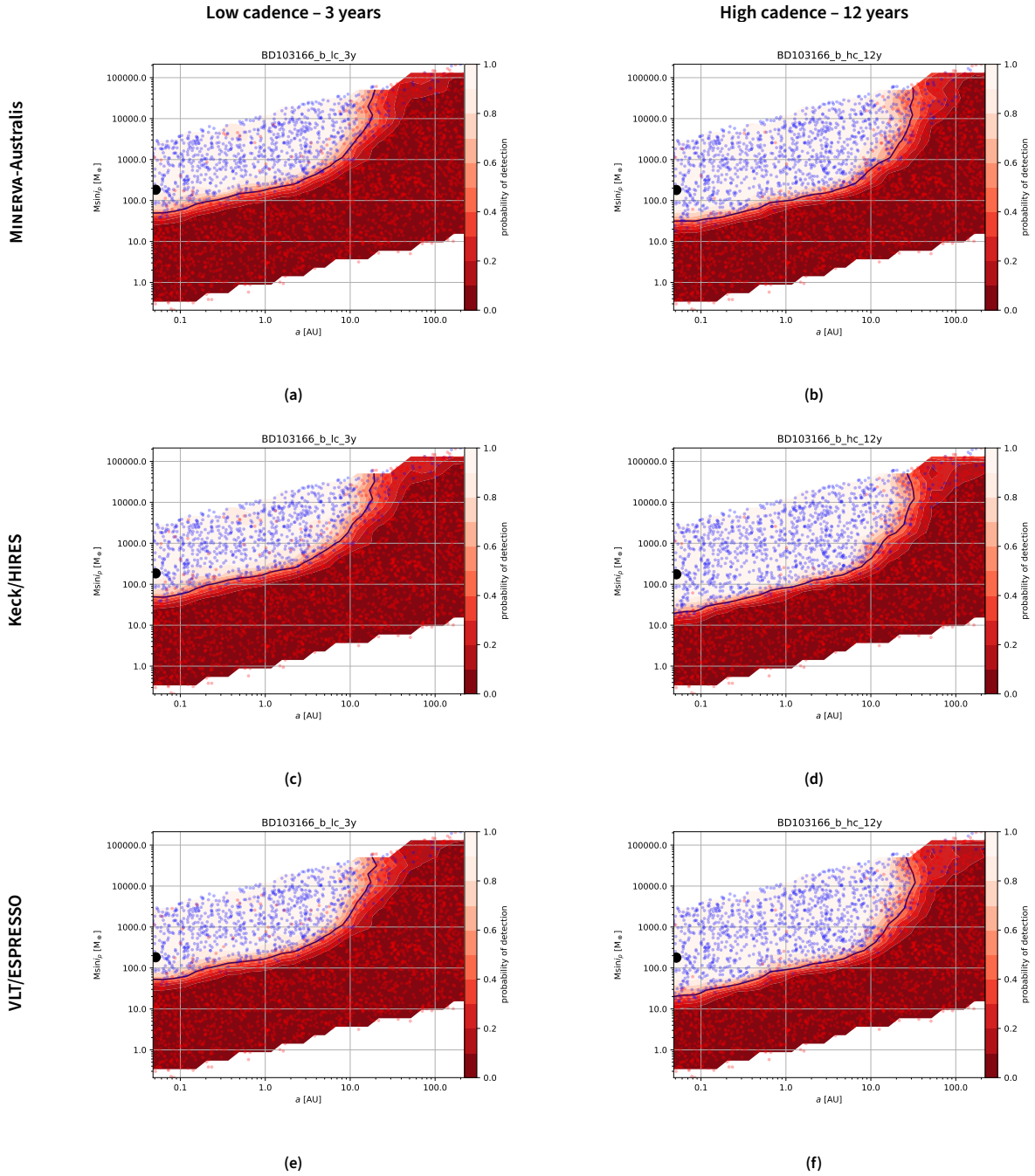


Figure 5. Comparison of different instruments and observing strategies. It can be noted that the line corresponding to 50% detection shifts downward and to the right as both the cadence and duration increase. Although subtle, differences are also seen between telescopes due to varying measurement precision.

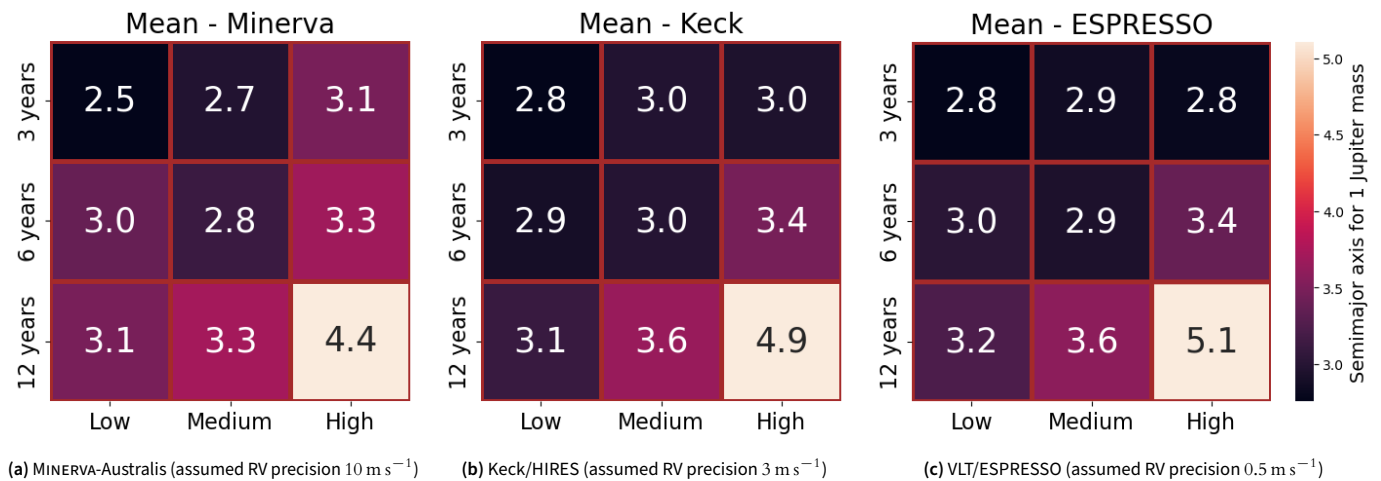


Figure 6. Cadence vs duration matrices showing the mean semi-major axis at which a $1 M_{\text{Jup}}$ planet was detectable 50% of the time for our simulated scenarios, based on the 28 stars in our sample. The three sub-figures (a, b, and c) present results for three exoplanet facilities - MINERVA-Australis, Keck/HIRES, and VLT/ESPRESSO, assuming mean RV precisions for those facilities of 10 , 3 and 0.5 m s^{-1} , respectively. In a given sub-figure, we show how the ability of each facility to detect Cold Jupiters is affected by different observation scenarios - temporal baselines for new observations of 3, 6, and 12 years (y-axis), and various observation cadences through that period (low, medium, and high cadence; x-axis). The colour and value of each tile gives the distance (in AU) at which the facility have a 50% chance of being able to detect a $1 M_{\text{Jup}}$ planet, averaged across our sample of 28 target stars. It is clear that the ability of each facility to detect such planets improves with higher observation cadence and longer baselines, as expected. Whilst increased RV precision yields some improvements in the detection distance, these improvements are somewhat less pronounced than might be expected.

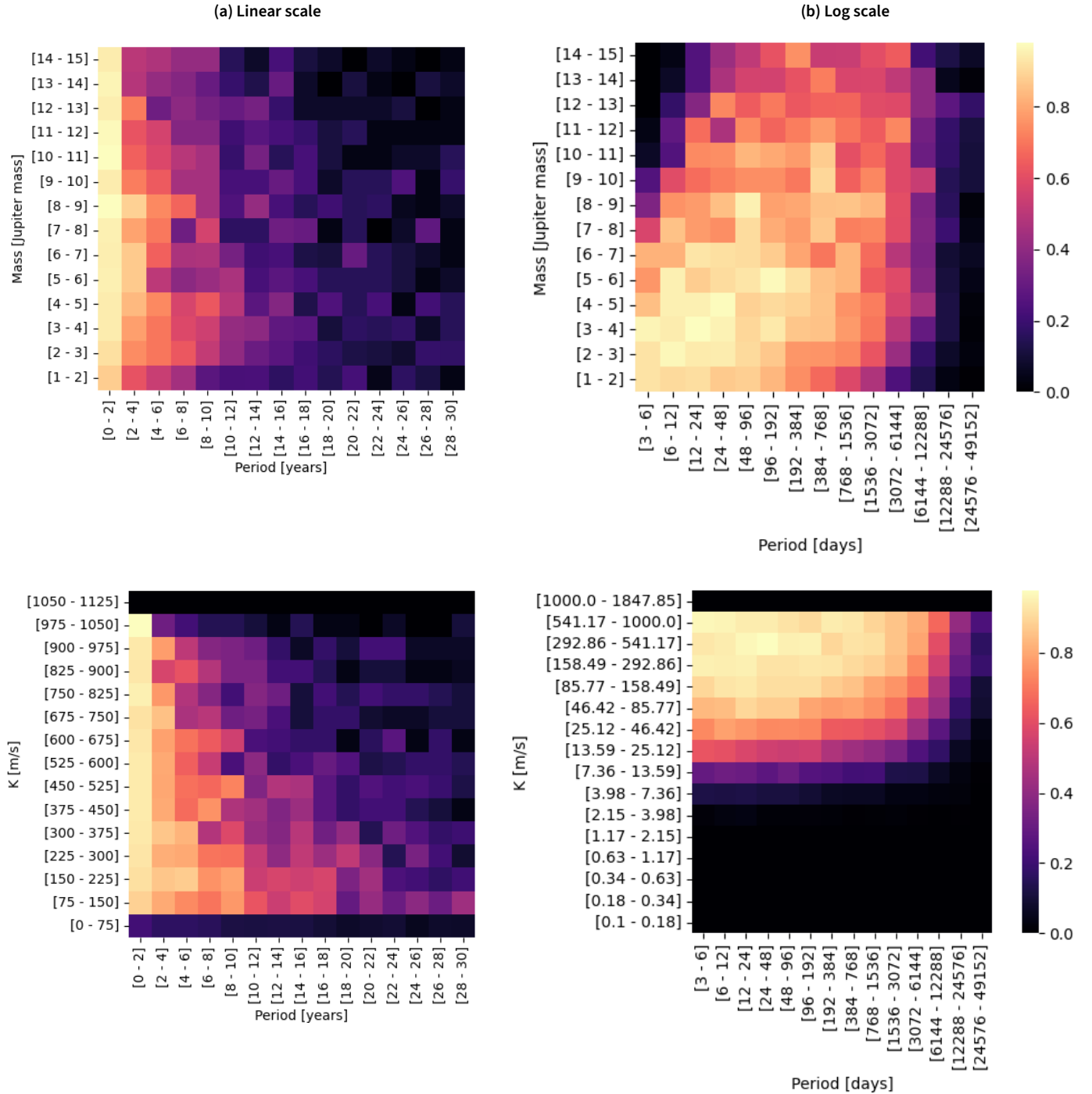
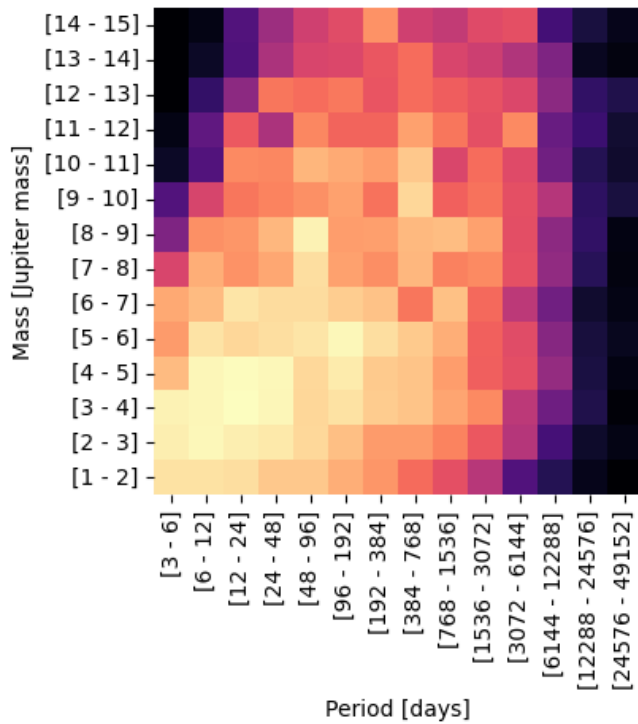
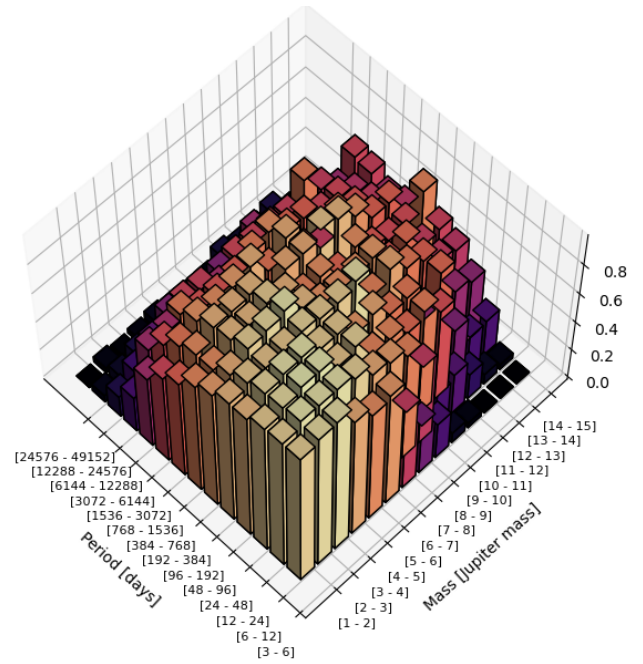


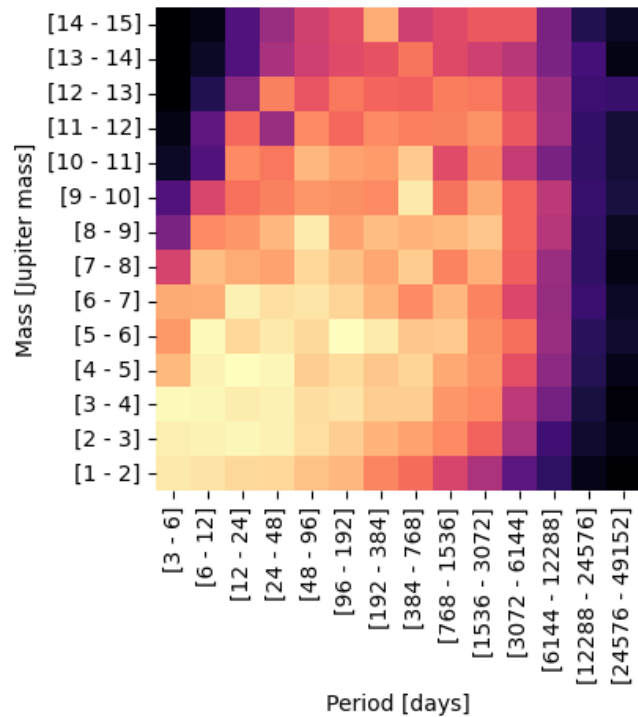
Figure 7. Heat maps showing the detection efficiency of a MINERVA-Australis class facility (RV precision 10m s^{-1}) for low cadence observations carried out over a period of three years (i.e. a short temporal baseline). The colour of each square reveals the mean detection probability for a planet in that particular mass and orbital period range, averaged over the 28 star systems studied in this work, based on simulated injection-recovery tests using 3000 injected planets. The lighter the colour, the greater the mean recovery rate. It is clear that the addition of just three years of low cadence data does not hugely improve our ability to detect Cold Jupiters over the current state of the data (presented in Figure 4), though some small gains are made. The upper panels show the data in planet mass vs orbital period space, whilst the lower ones show the same information plotted in terms of the observed radial velocity, K , and the orbital period of the planet in question. In the upper right panel, it appears that no planets are detected at very high mass for very short periods. This is an artefact of the injection-recovery process used, where *RVS* search only injects signals up to a radial velocity of 1000m s^{-1} . At the shortest orbital periods injected, this ceiling results in a maximum possible planet mass of $< 10M_J$ – and so that apparent void in detections is simply a location where no planets are injected. This ceiling is clearly seen in the lower right hand panel, showing that the highest velocity planets are very efficiently detected at short orbital periods, just as one would expect.



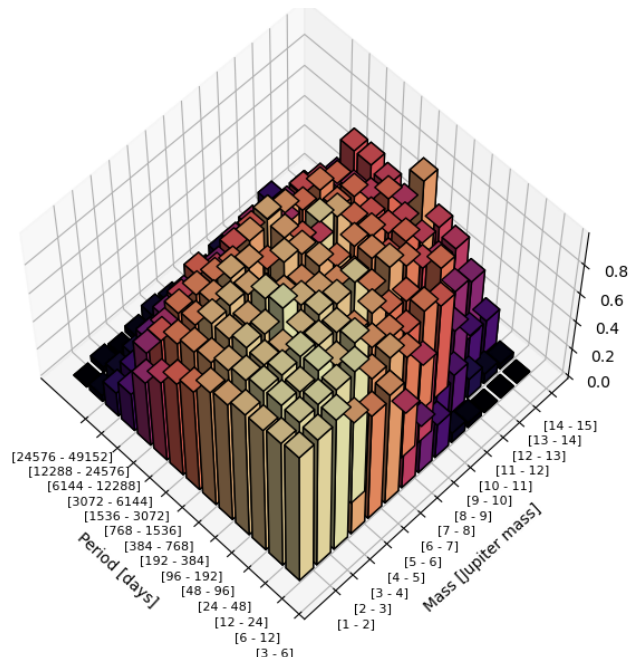
(a) Heatmap for VLT/ESPRESSO (low cadence – 3 y) (log scale)



(b) 3D representation

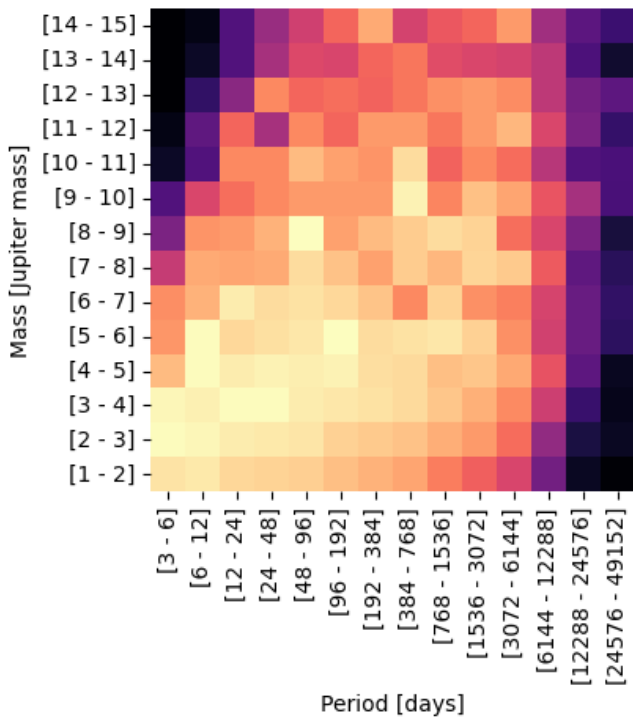


(c) Heatmap for VLT/ESPRESSO (medium cadence – 6 y) (log scale)

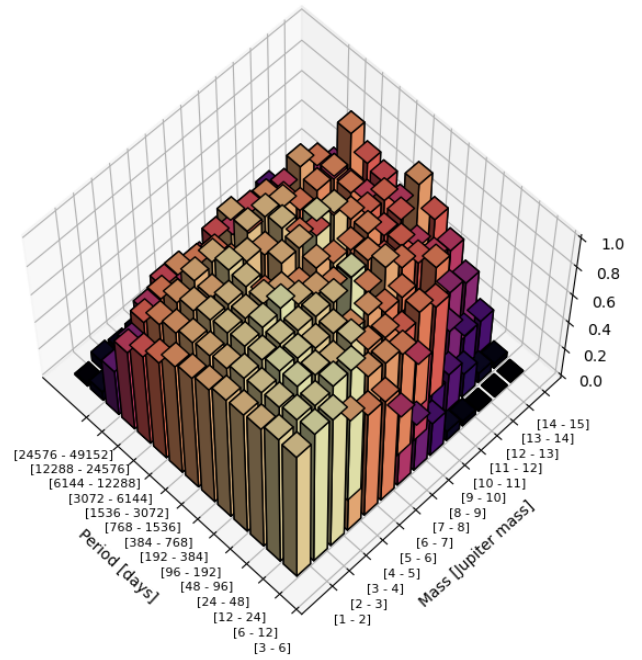


(d) 3D representation

Figure 8. Heat maps showing the efficiency with which a high-precision exoplanet survey (such as VLT/ESPRESSO) can detect exoplanets as a function of orbital period and planet mass, for three combinations of observation baseline and observation cadence. The left-hand column shows the data in two-dimensional plots, whilst the right-hand column presents the same results in a three-dimensional form, to help the reader visualise the regions where the ability of the facility to detect planets falls off. The valley at high-mass and short-period (the top left of the 2D maps) is artificial, being the result of the fact that the injection-recovery analysis using *RVS*search only considered RV signals with amplitudes between 0.1 and 1000 ms^{-1} – meaning that no extremely massive planets were injected at short orbital periods. Increasing both the observational cadence and baseline of observations clearly improves the efficiency with which Jupiter-analogue planets can be detected, with the most pronounced benefits coming at long orbital periods as a result of the longer baseline used. Data for the high-cadence 12-year observations are presented in Figure 9.



(a) Heat map for VLT/ESPRESSO (high cadence – 12 y) (log scale)



(b) 3D representation

Figure 9. Continuation of Figure 8, showing the heat map of detection efficiency for VLT/ESPRESSO observations using a high cadence for an observational baseline of 12 years, with the left panel showing a 2D representation of the data, and the right panel showing the same information in three dimensions.

Table 8. Table showing the semi-major axis at which a $1 M_J$ planet would have a 50% probability of detection around our 28 target stars, for observations carried out with a medium-precision exoplanet survey facility, such as Keck/HIRES, as a function of observational cadence and the baseline over which additional observations are carried out. As was the case for a low-precision facility (e.g. Table 7), a longer baseline of observations typically leads to Jupiter analogues being detectable on longer period orbits, with higher cadence observations typically resulting in an improvement in that detection distance over lower cadence observations.

	Low cadence			Medium cadence			High cadence		
	3 years	6 years	12 years	3 years	6 years	12 years	3 years	6 years	12 years
51Peg	5.85	5.85	5.89	5.73	5.87	6.08	5.87	5.91	6.42
BD-10 3166	2.84	3.05	4.2	3.13	4.14	6.4	3.42	5.77	8.65
HD102956	1.13	0.88	1.18	1.04	1.12	1.24	1.25	1.07	1.35
HD103720	2.56	2.17	2.57	2.56	2.46	2.56	2.36	2.78	4.36
HD103774	1.05	1.05	1.06	0.99	1.17	1.23	1.82	1.62	1.49
HD11231	0.1	0.1	0.48	0.47	0.55	1.01	0.85	1.11	2.84
HD118203	0.14	0.16	0.18	0.17	0.18	0.19	0.19	0.18	0.19
HD143105	0.52	0.48	0.55	0.52	0.55	0.56	0.59	0.63	0.84
HD149026	2.12	3.16	4.8	2.35	4.52	7.31	3.61	6.99	9.43
HD149143	2.87	2.82	2.73	2.82	3.01	4.43	3.07	3.28	3.34
HD162020	1.13	0.99	0.1	1.19	0.11	0.1	0.13	0.1	0.1
HD179949	1.15	1.15	1.15	1.15	1.2	1.17	1.15	1.18	1.08
HD185269	3.62	3.32	3.61	3.4	1.62	1.83	1.67	1.77	1.85
HD187123	9.57	9.03	10.15	10.97	9.79	9.03	9.97	9.03	7.29
HD189733	0.6	0.68	0.83	0.79	0.71	0.97	0.86	1.24	1.1
HD209458	5.7	6.08	6.31	6.18	6.25	6.76	6.01	6.37	7.41
HD212301	0.91	1.23	1.67	1.13	1.59	2.18	1.72	3.1	6.57
HD217107	6.49	8.51	8.34	8.12	9.31	8.83	8.56	9.83	9.4
HD2638	0.63	0.66	0.71	0.64	0.63	1.6	0.74	2.51	8.69
HD285507	1.14	1.14	0.93	0.87	1.29	3.81	1.87	2.01	5.99
HD68988	3.16	2.81	0.25	3.53	0.17	0.28	0.25	0.21	0.47
HD75289	5.05	4.68	5.82	4.36	5.07	7.38	4.9	6.25	7.42
HD83443	6.96	7.77	6.81	8.09	7.3	5.59	8.0	4.63	6.2
HD86081	1.19	1.19	0.8	1.2	1.1	1.45	1.55	2.66	9.75
HD88133	4.3	4.59	8.14	4.54	6.75	10.36	4.98	7.8	9.79
HIP14810	2.52	2.56	2.53	2.6	2.71	2.97	2.63	2.63	8.53
TauBoo	0.1	0.1	0.1	0.1	0.1	0.1	0.1	0.1	0.1
UpsAnd	2.16	2.42	2.17	2.01	2.04	2.14	1.95	2.33	2.6

Table 9. The semi-major axes at which a planet of mass $1 M_J$ would be detected with 50% probability orbiting our 28 target stars, for observations using a high-precision survey facility, such as VLT/ESPRESSO, as a function of observational cadence and the baseline over which observations are performed. As was the case for low- and medium-precision facilities, a longer baseline of observations again leads to Jupiter mass planets being detectable on longer period orbits, with higher cadence observations typically resulting in an improvement in that detection distance over lower cadence observations.

	Low cadence			Medium cadence			High cadence		
	3 years	6 years	12 years	3 years	6 years	12 years	3 years	6 years	12 years
51Peg	5.73	5.73	5.87	5.85	5.77	6.1	5.87	5.89	6.72
BD-10 3166	2.92	3.06	4.44	2.75	3.78	7.37	3.7	5.2	9.51
HD102956	0.97	0.84	1.0	1.16	0.75	1.12	1.06	1.34	1.22
HD103720	2.56	2.17	2.39	2.47	2.31	2.65	2.44	2.71	4.8
HD103774	0.99	1.05	1.0	0.98	1.04	1.22	1.06	1.63	1.65
HD11231	0.1	0.35	0.4	0.32	0.5	0.69	0.53	0.79	2.7
HD118203	0.14	0.15	0.17	0.17	0.19	0.19	0.19	0.17	0.21
HD143105	0.44	0.54	0.52	0.47	0.56	0.57	0.62	0.65	0.89
HD149026	2.31	4.9	5.51	2.6	4.49	8.07	2.91	7.06	8.77
HD149143	2.72	2.94	2.57	2.46	2.84	3.59	2.73	3.85	4.53
HD162020	1.09	1.0	0.1	1.19	0.11	0.1	0.13	0.1	0.1
HD179949	1.15	1.15	1.16	1.1	1.21	1.14	1.21	1.21	1.08
HD185269	3.63	3.32	3.59	3.4	1.66	1.84	1.73	1.82	1.79
HD187123	9.11	10.29	9.78	9.56	10.35	9.11	9.74	9.39	9.1
HD189733	0.57	0.64	0.69	0.74	0.79	0.87	0.82	1.23	1.09
HD209458	5.88	5.88	5.88	5.7	6.23	6.65	6.01	6.52	7.56
HD212301	0.84	1.37	1.81	1.34	1.88	2.62	2.04	2.23	5.72
HD217107	6.72	8.06	9.0	7.62	8.5	8.75	7.76	9.04	9.09
HD2638	0.65	0.68	0.74	0.62	0.61	1.56	0.69	2.59	8.39
HD285507	1.73	1.03	0.97	1.43	1.5	4.27	1.66	2.07	5.98
HD68988	2.99	3.01	3.11	3.32	0.18	0.17	0.19	0.22	0.33
HD75289	3.57	4.63	6.0	3.33	3.35	6.78	4.73	6.78	7.97
HD83443	7.57	7.95	7.44	8.39	7.95	5.75	7.36	5.4	6.7
HD86081	1.18	1.19	0.84	1.2	1.06	1.4	1.73	2.46	8.82
HD88133	4.26	4.56	6.76	4.5	6.89	9.39	5.19	7.46	11.76
HIP14810	2.52	2.73	2.83	2.6	2.59	2.88	2.99	2.63	9.02
TauBoo	0.1	0.1	0.1	0.1	0.1	0.1	0.1	0.1	2.53
UpsAnd	2.52	2.73	6.76	2.6	2.59	2.88	2.99	2.63	0.1

4.3 VLT/ESPRESSO/Minerva performance comparison

In the previous sections, we have considered the benefits of a variety of observational strategies in the search for Cold Jupiters for three different types of exoplanet search facilities – those with low radial velocity precision (analogues to the MINERVA-Australis array), with medium precision (like data obtained using Keck), and those with high precision (“extreme precision radial velocity” or “EPRV”) such as VLT/ESPRESSO). We have clearly shown that longer observational baselines are the key to detecting distant massive planets using radial velocity observations, regardless of the facility involved. Our results also reveal that increasing the observational cadence leads to the more efficient detection of Cold Jupiters in the vast majority of cases. In general, we also find that the use of high-precision facilities yields only marginal gains over the results obtained by smaller, more accessible telescopes (see e.g. Figure 6). In this section, we therefore address the question: can the long-term performance of large, highly accurate telescopes in the search for Jupiter-like planets be matched by smaller, more accessible, and more affordable facilities?

To address this, we consider our two extreme cases – VLT/ESPRESSO (high precision) and MINERVA-Australis (low precision). Rather than simply considering the detection efficiencies of the two facilities on their own, we look to make two direct comparisons. In the first, we calculate the ratio of successful detections made by VLT/ESPRESSO to those made using MINERVA-Australis – in other words, we divide the detection efficiency of one facility by the other. The results of this comparison are shown in Figure 10. In that Figure, a value of 1.0 denotes that the two facilities perform equally well. If the value is less than 1.0 (represented by reddish to black shades in the colour scale of Figure 10), then MINERVA-Australis outperforms VLT/ESPRESSO, whilst values greater than 1.0 (the lighter shades in Figure 10) denote VLT/ESPRESSO outperforming MINERVA-Australis. Looking at Figure 10, it is evident that both telescopes perform equally well across the majority of the phase-space considered. The right side of each plot initially appears to highlight areas where performance differences become significant, with numerous dark-shaded regions – particularly in the last column, which corresponds to high-cadence observations. The results in this region should, however, be treated with some caution. This is the region where the detection efficiencies for all three facilities are very low (as can be seen in Figures 7 and 8), and so the variation seen here is most likely simply noise.

The second comparison we make is to take the results calculated above (the ratio of the detection efficiencies of the two facilities), and scale the result by the ratio of the cost of the two facilities, as detailed in Equation 1. VLT/ESPRESSO^h is a high-performance but very expensive facility compared to MINERVA-Australisⁱ (European Southern Observatory, n.d.), and so it is interesting to consider the cost-effectiveness of the two types of facility as tools to search for Cold Jupiters.

$$\left(\frac{\$VLT/ESPRESSO}{\$Minerva} \right) \times \left(\frac{\#Minerva}{\#VLT/ESPRESSO} \right) \quad (1)$$

This equation equals 1 when MINERVA-Australis is as cost-effective as VLT/ESPRESSO, whilst values greater than 1 indicate that MINERVA-Australis provides better value for money (not in absolute performance, but in cost per detection). We present the results of this analysis in Figure 11, where it can be clearly seen that MINERVA-Australis represents a far more cost-effective tool for searching for Cold Jupiters than the more expensive facility. This is not a surprise – both facilities are broad equally efficient as tools for the detection of Cold Jupiters, and so it makes sense that the cheaper facility would be more cost-effective. Once again, the noisy results in the right hand columns in Figure 11 are purely the result of the low detection efficiencies for the two facilities at such long orbital periods.

Finally, we note some limitations to the simple comparison of cost-effectiveness we have described here. For example, the ESPRESSO approach clearly breaks down for very faint targets where smaller telescopes are unable to obtain useful RV data at all. Another subtlety we have not considered is a “hybrid” observing strategy whereby certain orbital phases disproportionately benefit from higher precision measurements. Such intricacies are beyond the scope of this work; it is clear that in practice, small and large telescopes serve complementary roles for this and other science goals.

5. Conclusions

In this work, we have defined Hot Jupiter-Cold Jupiter “siblings” as planetary systems containing both a Hot Jupiter and a distant outer giant. Motivated by the discovery of the Hot Jupiter-Cold Jupiter “siblings” in the HD 83443 system (Errico et al., 2022); we wished to estimate how common such architectures are, given the severe observational biases against detecting these sorts of systems. From a sample of 28 Hot Jupiter systems that had enough RV data to meaningfully contribute to this investigation, we indeed found the detection sensitivity woefully lacking, even for planets of many Jupiter masses. We then performed an extensive suite of simulated observational strategies to determine the way forward in addressing this problem.

Our analysis across nine scenarios and three telescopes reveals several key findings. First, the existing data, despite being gathered from well-studied and bright Hot Jupiter hosts, are generally ineffective at detecting cold Jupiters, highlighting the challenge of probing these longer-period companions. We suspect that this arises from a human bias: for Hot Jupiter systems, once the short-period planet is well-characterised, the target’s observing priority is reduced or eliminated in favour of other, “more interesting” targets. The result is that Hot Jupiter systems tend to have short baselines of RV data, hindering our quest to understand the occurrence of any planetary siblings.

We also find that, although higher instrumental precision extends sensitivity to larger semi-major axes for a given observ-

^hEstimated cost: USD 860,000,000

ⁱEstimated cost: USD 4,000,000

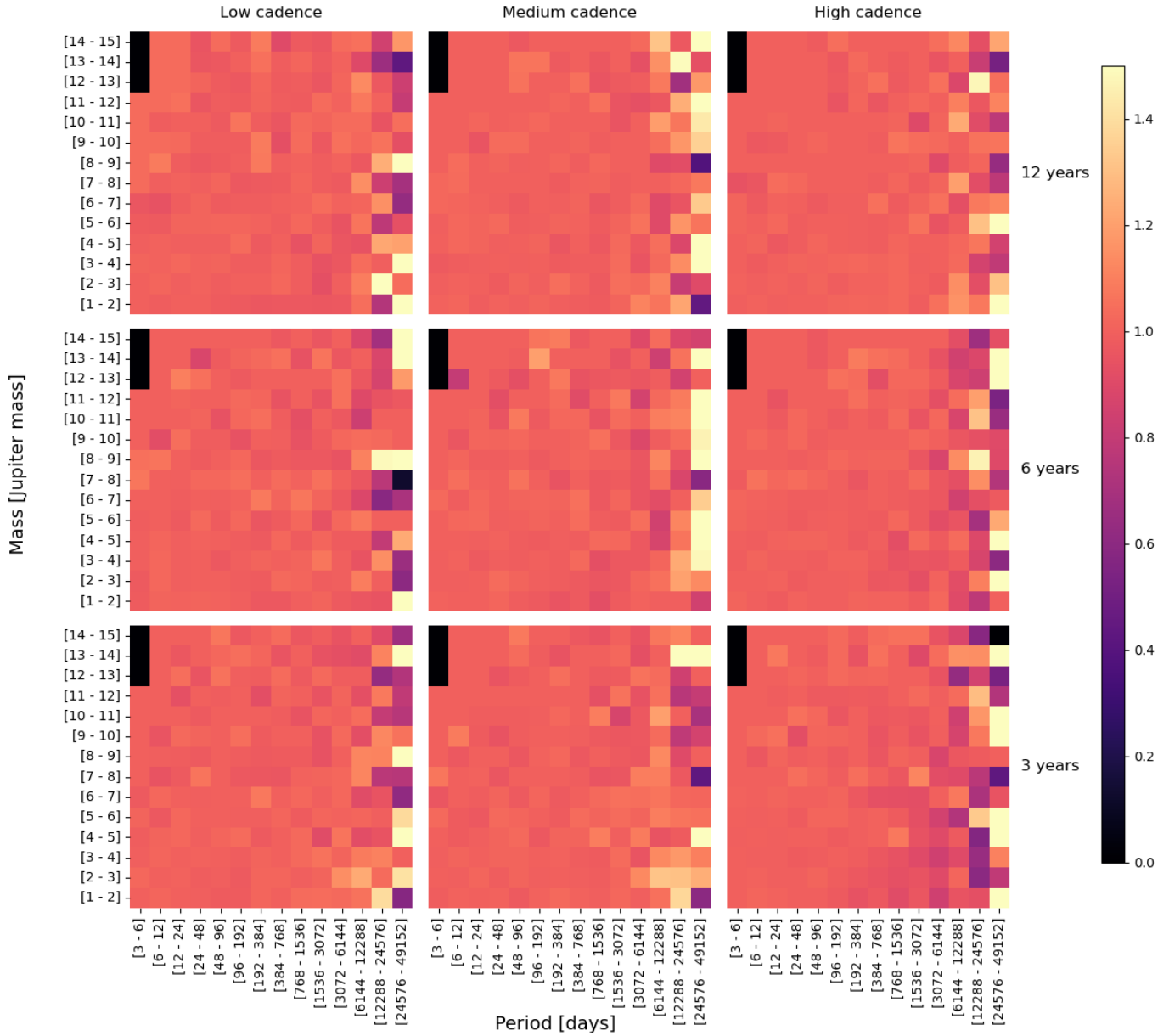


Figure 10. A direct comparison between the detection efficiencies of a low-precision facility (Minerva-Australis) and a high-precision facility (VLT/ESPRESSO), for the different observation scenarios considered in this work. Each square of each panel shows the ratio of the detection efficiencies of the two facilities – in other words, the efficiency of VLT/ESPRESSO divided by the efficiency of MINERVA-Australis at that point. Values greater than 1.0 show areas where VLT/ESPRESSO can more effectively detect massive planets than MINERVA-Australis, given the exact same observation strategy, whilst values less than 1.0 are areas where the smaller, cheaper facility proves to be more efficient. Other than at very long orbital periods (~ 6164 to ~ 24576 days), where VLT/ESPRESSO appears to be slightly more effective at medium cadence, and MINERVA-Australis performs slightly better at high cadence. The right-hand most columns are, however, regions of low detection efficiency for both facilities, meaning that the results displayed there are relatively noisy, and should be viewed with caution.

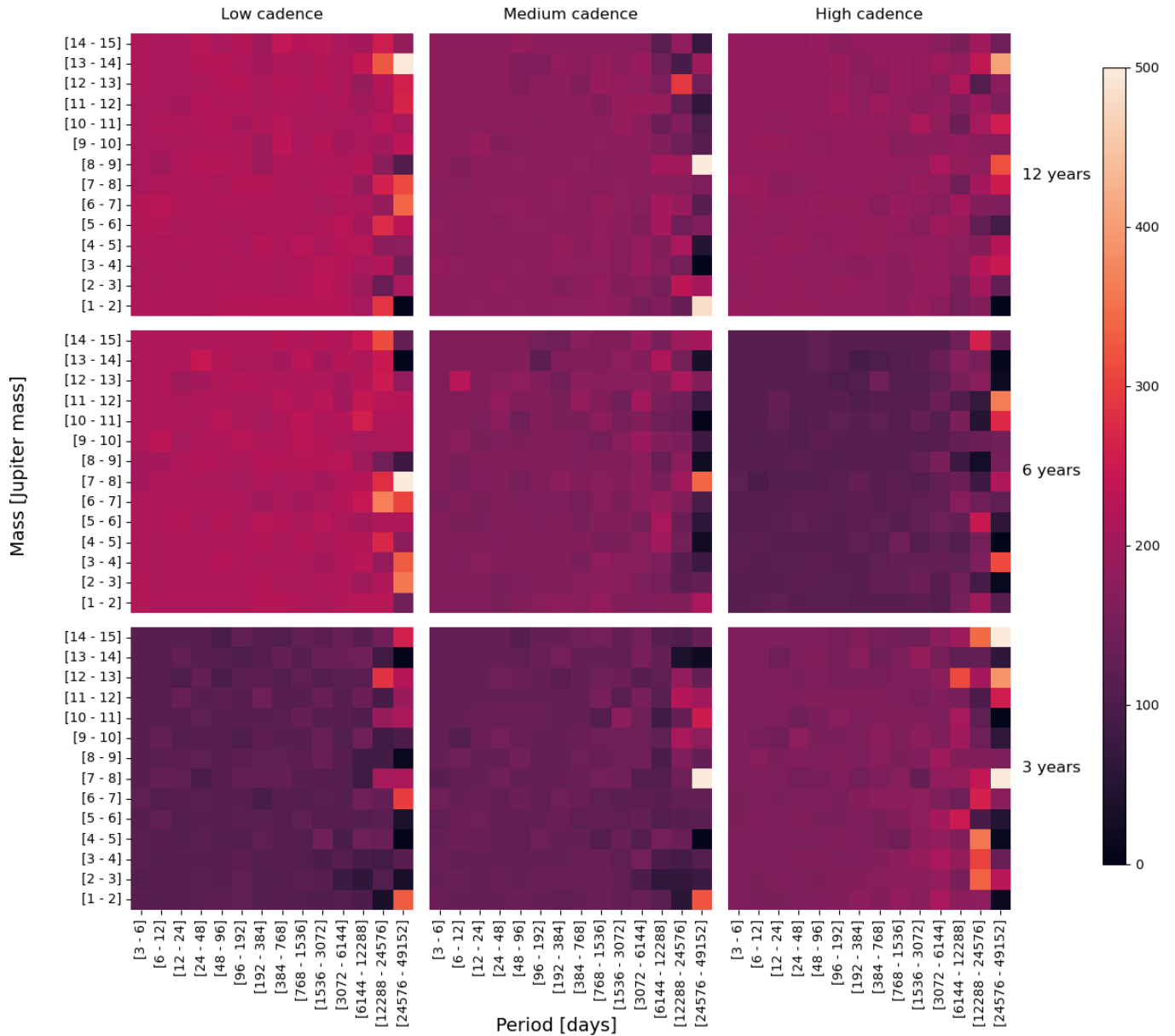


Figure 11. Figure showing the relative cost of detection for Cold Jupiters using a low resolution, low cost facility (such as MINERVA-Australis) compared to a high resolution, high cost facility such as VLT/ESPRESSO. This figure attempts to illustrate the most cost-effective method to search for massive planets orbiting other stars. Each panel plots the relative 'cost-effectiveness' of Cold Jupiter detections between these two facilities, for that particular observational scenario. A value of 500 (bright white) occurs when making a detection using VLT/ESPRESSO would come at a cost 500 times higher than the same detection using MINERVA-Australis; with the values in each box determined using equation 1. It is immediately apparent that the detection of Cold Jupiters is strikingly more cost-effective using facilities like MINERVA-AUSTRALIS, with the greatest difference between the cost-effectiveness being seen for the lowest observational cadences.

ing strategy, the total baseline over which an observation campaign is carried out is the dominant factor in our ability to detect cold Jupiters. We find that the results are relatively insensitive to the RV measurement precision of the facility being used; the performance of a high-cadence, decade-long program using a low-cost dedicated facility such as MINERVA-Australis matches, or even exceeds, that of shorter, lower-cadence observations by a higher cost extreme-precision RV (EPRV) facility such as VLT/ESPRESSO. Indeed, our results show that low-cost dedicated facilities such as MINERVA-Australis will prove to be far more cost-effective in delivering discoveries of Cold Jupiters than facilities such as Keck and VLT/ESPRESSO.

Notably, a high-cadence, decade-long Minerva program can match or exceed the performance of shorter, lower-cadence VLT/ESPRESSO observations, illustrating that modest measurement precision can be compensated for by strategic scheduling. A cost-normalised comparison further demonstrates that smaller, more accessible facilities can deliver superior return per dollar than flagship instruments when optimised for long-term monitoring. Our results emphasise the value of extended, regular RV campaigns for uncovering long-period exoplanets and inform the design of future surveys. This finding underscores the continuing relevance of traditional RV facilities in an era dominated by EPRV instruments.

Acknowledgements

The authors would like to express their sincere gratitude to the anonymous referee of this paper, whose comments and questions led to significant improvements in the manuscript.

MINERVA-Australis is supported by Australian Research Council LIEF Grant LE160100001, Discovery Grants DP180100972 and DP220100365, Mount Cuba Astronomical Foundation and institutional partners University of Southern Queensland, UNSW Sydney, MIT, Nanjing University, George Mason University, University of Louisville, University of California Riverside, University of Florida, and The University of Texas at Austin.

This publication makes use of The Data & Analysis Center for Exoplanets (DACE), which is a facility based at the University of Geneva (CH) dedicated to extrasolar planets data visualisation, exchange and analysis. DACE is a platform of the Swiss National Centre of Competence in Research (NCCR) PlanetS, federating the Swiss expertise in Exoplanet research. The DACE platform is available at <https://dace.unige.ch>.

This research has made use of the NASA Exoplanet Archive, which is operated by the California Institute of Technology, under contract with the National Aeronautics and Space Administration under the Exoplanet Exploration Program.

This work uses astropy (Astropy Collaboration et al., 2013, 2018, 2022), scipy (Virtanen et al., 2020), numpy (Harris et al., 2020), matplotlib (Hunter, 2007), pandas (pandas development team, 2020), seaborn (Waskom, 2021), Jupyter (<https://jupyter.org/>) and RVSearch (Rosenthal et al., 2021)

We respectfully acknowledge the traditional custodians of all lands throughout Australia, and recognise their continued cultural and spiritual connection to the land, waterways, cosmos, and community. We pay our deepest respects to all Elders, ancestors and descendants of the Giabal, Jarowair, and Kambuwal nations, upon whose lands the MINERVA-Australis facility at Mt Kent observatory is situated.

References

- Adams, E. R., Jackson, B., & Endl, M. 2016, *AJ*, 152, 47
- Addison, B., Wright, D. J., Wittenmyer, R. A., et al. 2019, *Publications of the Astronomical Society of the Pacific*, 131, 115003
- Addison, B. C., Wright, D. J., Nicholson, B. A., et al. 2021, *MNRAS*, 502, 3704
- Airapetian, V. S., Barnes, R., Cohen, O., et al. 2020, *International Journal of Astrobiology*, 19, 136
- Astropy Collaboration, Robitaille, T. P., Tollerud, E. J., et al. 2013, *A&A*, 558, A33
- Astropy Collaboration, Price-Whelan, A. M., Sipőcz, B. M., et al. 2018, *AJ*, 156, 123
- Astropy Collaboration, Price-Whelan, A. M., Lim, P. L., et al. 2022, *ApJ*, 935, 167
- Bonomo, A. S., Dumusque, X., Massa, A., et al. 2023, arXiv e-prints, arXiv:2304.05773
- Bouchy, F., Udry, S., Mayor, M., et al. 2005, *A&A*, 444, L15
- Bryan, M. L., Knutson, H. A., Howard, A. W., et al. 2016, *ApJ*, 821, 89
- Bryson, S., Kunimoto, M., Kopparapu, R. K., et al. 2021, *AJ*, 161, 36
- Butler, R. P., Marcy, G. W., Vogt, S. S., & Apps, K. 1998, *PASP*, 110, 1389
- Butler, R. P., Marcy, G. W., Williams, E., Hauser, H., & Shirts, P. 1997, *ApJ*, 474, L115
- Butler, R. P., Tinney, C., Marcy, G. W., et al. 2001, *The Astrophysical Journal*, 555, 410
- Butler, R. P., Tinney, C. G., Marcy, G. W., et al. 2001, *ApJ*, 555, 410
- Butler, R. P., Vogt, S. S., Marcy, G. W., et al. 2000, *ApJ*, 545, 504
- Butler, R. P., Marcy, G. W., Vogt, S. S., et al. 2002, *ApJ*, 578, 565
- Butler, R. P., Wright, J. T., Marcy, G. W., et al. 2006, *ApJ*, 646, 505
- Butler, R. P., Vogt, S. S., Laughlin, G., et al. 2017, *The Astronomical Journal*, 153, 208
- Cannon, A. J., & Pickering, E. C. 1993, *VizieR Online Data Catalog: Henry Draper Catalogue and Extension (Cannon+ 1918-1924; ADC 1989)*, *VizieR On-line Data Catalog: III/135A*. Originally published in: *Harv. Ann.* 91-100 (1918-1924)
- Castro-González, A., Lillo-Box, J., Correia, A. C. M., et al. 2024, *A&A*, 684, A160
- Charbonneau, D., Brown, T. M., Latham, D. W., & Mayor, M. 2000, *ApJ*, 529, L45
- Christiansen, J. L., McElroy, D. L., Harbut, M., et al. 2025, *PSJ*, 6, 186
- Cumming, A., Butler, R. P., Marcy, G. W., et al. 2008, *PASP*, 120, 531
- da Silva, R., Udry, S., Bouchy, F., et al. 2006, *A&A*, 446, 717
- Dressing, C. D., & Charbonneau, D. 2015, *ApJ*, 807, 45
- Errico, A., Wittenmyer, R. A., Horner, J., et al. 2022, *AJ*, 163, 273
- European Southern Observatory. n.d., *FAQ – VLT and Paranal*, <https://www.eso.org/public/about-eso/faq/faq-vlt-paranal/#25>, accessed: 27 April 2025
- Feng, Y. K., Wright, J. T., Nelson, B., et al. 2015, *ApJ*, 800, 22
- Fischer, D. A., Marcy, G. W., Butler, R. P., Vogt, S. S., & Apps, K. 1999a, *PASP*, 111, 50
- . 1999b, *PASP*, 111, 50
- Fischer, D. A., Marcy, G. W., Butler, R. P., et al. 2003, *ApJ*, 586, 1394
- Fischer, D. A., Laughlin, G., Butler, P., et al. 2005, *ApJ*, 620, 481
- Fischer, D. A., Laughlin, G., Marcy, G. W., et al. 2006, *ApJ*, 637, 1094
- Fujii, Y., Angerhausen, D., Deitrick, R., et al. 2018, *Astrobiology*, 18, 739
- Fulton, B. J., Petigura, E. A., Blunt, S., & Sinukoff, E. 2018, *Publications of the Astronomical Society of the Pacific*, 130, 044504
- Gan, T., Guo, K., Liu, B., et al. 2024, *ApJ*, 967, 74
- Gilbert, E. A., Vanderburg, A., Rodriguez, J. E., et al. 2023, *ApJ*, 944, L35
- Gillon, M., Triaud, A. H. M. J., Demory, B.-O., et al. 2017, *Nature*, 542, 456
- Gomes, R., Levison, H. F., Tsiganis, K., & Morbidelli, A. 2005, *Nature*, 435, 466
- Gray, R. O., Napier, M. G., & Winkler, L. I. 2001, *AJ*, 121, 2148
- Grazier, K. R. 2016, *Astrobiology*, 16, 23
- Grieves, N., Ge, J., Thomas, N., et al. 2018, *MNRAS*, 481, 3244
- Harada, C. K., Dressing, C. D., Kane, S. R., & Ardestani, B. A. 2024a, *ApJS*, 272, 30
- Harada, C. K., Dressing, C. D., Kane, S. R., et al. 2024b, arXiv e-prints, arXiv:2409.10679
- Harris, C. R., Millman, K. J., van der Walt, S. J., et al. 2020, *Nature*, 585, 357
- Haswell, C. A., Staab, D., Barnes, J. R., et al. 2020, *Nature Astronomy*, 4, 408
- Hébrard, G., Arnold, L., Forveille, T., et al. 2016, *A&A*, 588, A145
- Henry, G. W., Marcy, G. W., Butler, R. P., & Vogt, S. S. 2000, *ApJ*, 529, L41
- Horner, J., & Jones, B. W. 2008, *International Journal of Astrobiology*, 7, 251
- . 2009, *International Journal of Astrobiology*, 8, 75
- . 2010, *International Journal of Astrobiology*, 9, 273
- . 2012, *International Journal of Astrobiology*, 11, 147
- Horner, J., Jones, B. W., & Chambers, J. 2010, *International Journal of Astrobiology*, 9, 1
- Horner, J., Mousis, O., Petit, J. M., & Jones, B. W. 2009, *Planet. Space Sci.*, 57, 1338
- Horner, J., Vervoort, P., Kane, S. R., et al. 2020a, *AJ*, 159, 10
- Horner, J., Kane, S. R., Marshall, J. P., et al. 2020b, *PASP*, 132, 102001
- Howard, A. W., & Fulton, B. J. 2016, *PASP*, 128, 114401
- Hunter, J. D. 2007, *Computing in Science & Engineering*, 9, 90
- Johnson, J. A., Marcy, G. W., Fischer, D. A., et al. 2006a, *ApJ*, 652, 1724
- . 2006b, *ApJ*, 647, 600
- Johnson, J. A., Bowler, B. P., Howard, A. W., et al. 2010, *ApJ*, 721, L153
- Kipping, D. M. 2013, *MNRAS*, 434, L51
- Knutson, H. A., Fulton, B. J., Montet, B. T., et al. 2014, *ApJ*, 785, 126
- Kraus, A. L., & Hillenbrand, L. A. 2007, *AJ*, 134, 2340
- Kunimoto, M., & Matthews, J. M. 2020a, *AJ*, 159, 248
- . 2020b, *AJ*, 159, 248
- Lagrange, A. M., Philipot, F., Rubini, P., et al. 2023, *A&A*, 677, A71
- Lalotis, K., Burt, J. A., Mamajek, E. E., et al. 2023, *AJ*, 165, 176
- Levison, H. F., Morbidelli, A., Tsiganis, K., Nesvorný, D., & Gomes, R. 2011, *AJ*, 142, 152
- Li, Z., Kane, S. R., Blunt, S., & Harada, C. K. 2025, arXiv e-prints, arXiv:2509.17169
- Lo Curto, G., Mayor, M., Clausen, J. V., et al. 2006, *A&A*, 451, 345
- Lo Curto, G., Mayor, M., Benz, W., et al. 2013, *A&A*, 551, A59
- Lo Curto, G., Pepe, F., Avila, G., et al. 2015, *The Messenger*, 162, 9
- Maciejewski, G., Niedzielski, A., Goździewski, K., et al. 2024, *A&A*, 688, A172
- Malavolta, L., Nascimbeni, V., Piotto, G., et al. 2016, *A&A*, 588, A118
- Marcy, G. W., Butler, R. P., Williams, E., et al. 1997, *ApJ*, 481, 926
- Mayor, M., & Queloz, D. 1995, *Nature*, 378, 355
- Morbidelli, A., Chambers, J., Lunine, J. I., et al. 2000, *Meteoritics & Planetary Science*, 35, 1309
- Moutou, C., Mayor, M., Bouchy, F., et al. 2005, *A&A*, 439, 367
- Moutou, C., Curto, G. L., Mayor, M., et al. 2015, *Astronomy & Astrophysics*, 576, A48
- Naef, D., Mayor, M., Beuzit, J. L., et al. 2004, *A&A*, 414, 351
- Naef, D., Mayor, M., Pepe, F., et al. 2001, *A&A*, 375, 205
- Nesvorný, D. 2018, *ARA&A*, 56, 137
- Nielsen, E. L., De Rosa, R. J., Macintosh, B., et al. 2019, *AJ*, 158, 13
- O'Brien, D. P., Walsh, K. J., Morbidelli, A., Raymond, S. N., & Mandell, A. M. 2014, *Icarus*, 239, 74
- Owen, T., & Bar-Nun, A. 1995, *Icarus*, 116, 215
- pandas development team, T. 2020, *pandas-dev/pandas: Pandas*, doi:10.5281/zenodo.3509134
- Pepe, F., Molaro, P., Cristiani, S., et al. 2014, *Astronomische Nachrichten*, 335, 8
- Perryman, M. 2018, *The exoplanet handbook* (Cambridge University Press)
- Polanski, A. S., Lubin, J., Beard, C., et al. 2024, *ApJS*, 272, 32
- Poleski, R., Skowron, J., Mróz, P., et al. 2021, *Acta Astron.*, 71, 1
- Quinn, S. N., White, R. J., Latham, D. W., et al. 2014, *ApJ*, 787, 27

- Raymond, S. N., & Izidoro, A. 2017, *Icarus*, 297, 134
- Rosenthal, L. J., Fulton, B. J., Hirsch, L. A., et al. 2021, *ApJS*, 255, 8
- Salz, M., Schneider, P. C., Czesla, S., & Schmitt, J. H. M. M. 2015, *A&A*, 576, A42
- Sato, B., Fischer, D. A., Henry, G. W., et al. 2005, *ApJ*, 633, 465
- Schwieterman, E. W., Kiang, N. Y., Parenteau, M. N., et al. 2018, *Astrobiology*, 18, 663
- Sousa, S. G., Adibekyan, V., Delgado-Mena, E., et al. 2021, *A&A*, 656, A53
- Stassun, K. G., Collins, K. A., & Gaudi, B. S. 2017, *AJ*, 153, 136
- Swift, J. J., Bottom, M., Johnson, J. A., et al. 2015, *Journal of Astronomical Telescopes, Instruments, and Systems*, 1, 027002
- Tinney, C., Butler, R. P., Marcy, G. W., et al. 2001, *The Astrophysical Journal*, 551, 507
- Tinney, C. G., Butler, R. P., Marcy, G. W., et al. 2001, *ApJ*, 551, 507
- TriAUD, A. H. M. J., Queloz, D., Bouchy, F., et al. 2009, *A&A*, 506, 377
- TriAUD, A. H. M. J., Neveu-VanMalle, M., Lendl, M., et al. 2017, *MNRAS*, 467, 1714
- Trifonov, T., Tal-Or, L., Zechmeister, M., et al. 2020, *A&A*, 636, A74
- Udry, S., Mayor, M., Naef, D., et al. 2002, *A&A*, 390, 267
- Udry, S., Mayor, M., Queloz, D., Naef, D., & Santos, N. 2000, in *From Extrasolar Planets to Cosmology: The VLT Opening Symposium*, ed. J. Bergeron & A. Renzini, 571
- Van Zandt, J., Petigura, E. A., Lubin, J., et al. 2025, *AJ*, 169, 235
- Vanderburg, A., Rowden, P., Bryson, S., et al. 2020, *ApJ*, 893, L27
- Vervoort, P., Horner, J., Kane, S. R., Kirtland Turner, S., & Gilmore, J. B. 2022, *AJ*, 164, 130
- Virtanen, P., Gommers, R., Oliphant, T. E., et al. 2020, *Nature Methods*, 17, 261
- Vogt, S. S., Butler, R. P., Marcy, G. W., et al. 2005a, *ApJ*, 632, 638
- . 2005b, *ApJ*, 632, 638
- . 2002, *ApJ*, 568, 352
- Vogt, S. S., Marcy, G. W., Butler, R. P., & Apps, K. 2000, *ApJ*, 536, 902
- Vogt, S. S., Allen, S. L., Bigelow, B. C., et al. 1994, in *Society of Photo-Optical Instrumentation Engineers (SPIE) Conference Series*, Vol. 2198, *Instrumentation in Astronomy VIII*, ed. D. L. Crawford & E. R. Craine, 362
- Waltham, D. 2019, *Earth Science Reviews*, 192, 445
- Waskom, M. L. 2021, *Journal of Open Source Software*, 6, 3021
- Weiss, L. M., Isaacson, H., Howard, A. W., et al. 2024, *ApJS*, 270, 8
- Wetherill, G. W. 1994, *Ap&SS*, 212, 23
- . 1995, *Nature*, 373, 470
- Wilson, M. L., Eastman, J. D., Cornachione, M. A., et al. 2019, *PASP*, 131, 115001
- Wittenmyer, R. A., Endl, M., & Cochran, W. D. 2007, *ApJ*, 654, 625
- Wittenmyer, R. A., Errico, A., Holt, T. R., et al. 2025, *MNRAS*, 539, 457
- Wittenmyer, R. A., Horner, J., Carter, B. D., et al. 2018, *arXiv e-prints*, arXiv:1806.09282
- Wittenmyer, R. A., Tinney, C., Butler, R., et al. 2011b, *The Astrophysical Journal*, 738, 81
- Wittenmyer, R. A., Tinney, C., O'Toole, S. J., et al. 2011a, *The Astrophysical Journal*, 727, 102
- Wittenmyer, R. A., Welsh, W. F., Orosz, J. A., et al. 2005, *ApJ*, 632, 1157
- Wittenmyer, R. A., Tinney, C. G., Horner, J., et al. 2013, *PASP*, 125, 351
- Wittenmyer, R. A., Horner, J., Tinney, C. G., et al. 2014, *ApJ*, 783, 103
- Wittenmyer, R. A., Butler, R. P., Tinney, C., et al. 2016, *The Astrophysical Journal*, 819, 28
- Wittenmyer, R. A., Wang, S., Horner, J., et al. 2020, *MNRAS*, 492, 377
- Wolszczan, A. 1994, *Science*, 264, 538
- Wolszczan, A., & Frail, D. A. 1992, *Nature*, 355, 145
- Wright, J. T., Upadhyay, S., Marcy, G. W., et al. 2009, *ApJ*, 693, 1084
- Zechmeister, M., Kürster, M., Endl, M., et al. 2013, *Astronomy & Astrophysics*, 552, A78
- Zhang, J., Weiss, L. M., Huber, D., et al. 2025, *AJ*, 169, 200
- Zhu, W., Petrovich, C., Wu, Y., Dong, S., & Xie, J. 2018a, *ApJ*, 860, 101
- . 2018b, *ApJ*, 860, 101
- Zink, J. K., & Howard, A. W. 2023, *ApJ*, 956, L29